RSC Advances

PAPER

View Article Online
View Journal | View Issue

Check for updates

Cite this: *RSC Adv.*, 2021, **11**, 29354

Deciphering the interaction of flavones with calf thymus DNA and octamer DNA sequence $(CCAATTGG)_2$†

Shailendra Kumar and Maya S. Nair *

We investigated the interaction of three flavone compounds, baicalein, chrysin and flavone with calf thymus DNA and octamer DNA sequence $(CCAATTGG)_2$. The binding mechanisms of the flavone compounds with both DNA were unveiled using biophysical, thermodynamic and molecular modelling techniques. Absorption and fluorescence titrations confirm the formation of the DNA complexes along with the extent of interaction. Absorption data proposed an intercalation mode of binding. Fluorescence displacement assays using ethidium bromide and Hoechst 33258 data supports a partial intercalation. Potassium iodide quenching substantiated this finding. Circular dichroism data revealed major structural changes on binding with flavones which can arise from intercalation partially or in a tilted arrangement. Analysis of the effect of ionic strength on complex formation eliminated the role of electrostatic interaction in the binding. Differential scanning calorimetric data showed substantial changes in the melting temperatures of complexes and predicted the DNA–baicalein complex as the most stable one. Molecular modelling showcased that the complexes are located near the AT rich region. Docking analysis with different sequences showed that the flavone compounds intercalated with base pairs only with $d(CGATCG)_2$.

Received 26th May 2021
Accepted 22nd August 2021

DOI: 10.1039/d1ra04101k

rsc.li/rsc-advances

Open Access Article. Published on 01 September 2021. Downloaded on 4/7/2026 8:03:30 PM.
This article is licensed under a Creative Commons Attribution-NonCommercial 3.0 Unported Licence.

1. Introduction

Small molecule–DNA interaction is an exciting research area that resulted in the identification of many therapeutic molecules. Many anticancer and antitumor drug molecules find DNA as the primary target. Different therapeutic agents' mode of action discovers them either as intercalator or groove binding molecules.[1–6]

Several anticancer agents bind to DNA intercalatively causing structural perturbations in DNA, thereby restricting the DNA from binding to its respective targets.[7] Groove binding molecules do not produce significant distortions in the DNA structure but can inhibit binding to many proteins, thereby blocking many cellular processes.[1,8,9] Knowledge about the small molecule interaction mechanism with DNA can enlighten the strategy for designing compounds with better binding efficacy and pharmacological potential.

Many molecules derived from natural products are being used as drugs and many naturally available compounds are potential therapeutic agents.[10–12] Flavones, a class of flavonoids possessing pharmacological values, are secondary metabolites in plants. Flavones are distinguished by the number and position of the hydroxyl group on the phenyl rings (Fig. 1). The simplest compound in this class is flavone. Baicalein and chrysin are two other molecules in this subgroup of flavonoids.[13] Baicalein, chrysin and flavone are known to possess various biological and pharmaceutical functions such as anti-inflammatory, antimicrobial, antiviral, anticancer and radical scavenging activities, as evidenced from several studies reported.[14–20] These properties can be attributed to their association with different macromolecules, *viz*, proteins, enzymes and nucleic acids, available in the cell. Among these, nucleic acids are one of the primary targets. Studies on flavone–DNA interaction have been reported by many researchers and are of great research interest.

Structure–activity relationship studies on baicalein, chrysin and wogonin with calf thymus DNA (CT DNA) showed that the

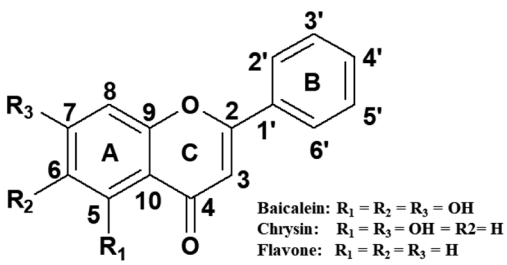

Fig. 1 Structure of flavone.

Department of Biosciences and Bioengineering, Indian Institute of Technology Roorkee, Roorkee, Uttarakhand-247667, India. E-mail: maya.nair@bt.iitr.ac.in; mayasfbt@iitr.ac.in; Fax: +91-1332-273560; Tel: +91-1332-285790

† Electronic supplementary information (ESI) available. See DOI: 10.1039/d1ra04101k

© 2021 The Author(s). Published by the Royal Society of Chemistry

Open Access Article. Published on 01 September 2021. Downloaded on 4/7/2026 8:03:30 PM.
This article is licensed under a Creative Commons Attribution-NonCommercial 3.0 Unported Licence.

three flavones intercalate between the DNA base pairs.[13,21,22] Another report suggests that baicalein can detect DNA at a concentration level of 4.1×10^{-8} g ml^{-1} and binds to DNA in a groove binding style.[23] Interaction studies of baicalein, wogonin and baicalin with fish sperm DNA revealed the intercalation mode of binding.[24] Vitorino *et al.*[13] reported the interaction of flavone and a few hydroxy flavones with CT DNA and found the compounds intercalated into the DNA double helix. These studies, therefore, put forth different modes of interaction between flavones with DNA. Consequently, it is interesting to revisit the interaction of few flavone compounds with DNA.

The present study investigates the interaction of CT DNA and an octamer DNA sequence d(CCAATTGG)$_2$ with baicalein, chrysin and flavone using absorption, fluorescence, circular dichroism and thermal studies through differential scanning calorimetry. An attempt has been made to explore the binding coefficients, binding mode and binding affinities of these compounds with both forms of DNA. CT DNA was a model DNA with many base pairs and no sequence specificity. The octamer sequence d(CCAATTGG)$_2$ was chosen as the CCAATTGG motif is widely present in the promoter region of human, fly and rat genomes responsible for controlling the regulatory pathways of many growth factors, tumour suppressor genes and oncogenes.[25–27] CCAAT sequence is also present in the promoter region of many oncogenes.[28–30] Therefore, the interaction of the flavone compounds with this sequence can shed light on the compounds' sequence-specific binding.

2. Materials and methods

Calf thymus DNA, oligonucleotide sequence CCAATTGG, baicalein, chrysin, flavone, ethidium bromide, Hoechst 33258 were procured from Sigma Aldrich Co., USA. The DNA samples were prepared in 20 mM sodium phosphate buffer containing 0.2 mM EDTA and 10 mM sodium chloride at pH 7. The oligonucleotide sequence was heated at 95 °C for 5 minutes and left at room temperature for the proper annealing. Baicalein was dissolved in dimethyl sulfoxide, chrysin and flavone were dissolved in methanol. The concentrations of d(CCAATTGG)$_2$ DNA sequence (molar extinction coefficient ε = 76 300 M^{-1} cm^{-1}) and calf thymus DNA (ε = 6600 M^{-1} cm^{-1}) were determined spectrophotometrically. Dilutions were made in the buffer. Other chemicals used were of analytical grade, and Millipore water was used.

2.1 Absorption studies

Absorption experiments were done using a CARY 60 spectrophotometer (Agilent Technologies). Spectra were recorded from 200 to 800 nm using a 1 cm pathlength quartz cuvette. 20 μM solutions of flavone compounds were titrated with increasing DNA concentrations to get different ratios R (DNA to flavones, N/D = R). The baseline subtraction was done to correct the background with the appropriate buffer solution. Binding coefficient K_b was calculated using Scatchard equation and described in Section 3.1.2.

2.2 Fluorescence studies

Fluorescence measurements were carried out on a FluoroMax plus spectrofluorometer (Horiba Scientific, USA). DNA solutions were gradually added in steps to a 20 μM flavones solution at room temperature. Spectra were recorded with excitation wavelengths set at 336 nm, 326 nm and 302 nm for baicalein, chrysin and flavone, respectively and emission spectra were scanned from 320 to 650 nm. Excitation and emission slits were kept at 5 nm. Emission intensities were corrected for absorption of the excitation light and re-absorption of the emitted light to decrease the inner filter effect.

2.3 Competitive displacement assay

This method is helpful to determine the binding mode between DNA and small molecules. A solution containing 1 μM of EtBr or Hoechst 33258 and 20 μM of DNA concentration was titrated with increasing flavones concentrations (0–50 μM) in displacement assay. The EtBr–DNA complex was excited at 476 nm and emission spectra were recorded from 500 nm to 750 nm. For the Hoechst–DNA system, excitation was set at 343 nm, and emission was monitored from 350 to 650 nm.

2.4 Quenching studies

Fluorescence quenching studies were performed with the anionic quencher potassium iodide (KI) in the absence and presence of d(CCAATTGG)$_2$ and CT DNA. Experiments were conducted with 20 μM concentration of flavones and 40 μM of DNA. Fluorescence intensities of flavones were monitored by changing the concentration of KI (0–13 mM). Data were plotted with relative fluorescence intensity (F_0/F) *versus* KI. Fluorescence quenching constants (K_{sv}) were deduced from the Stern–Volmer quenching equation,

$$\frac{F_0}{F} = 1 + K_{sv}[Q]$$

where F_0 and F are the fluorescence intensities in the absence and presence of quencher, [Q], the quencher concentration, and K_{sv} is the quenching constant.

2.5 Effect of ionic strength

The effect of ionic strength on the DNA–flavone complexes was evaluated by monitoring the variations in fluorescence intensities of flavone compounds with different concentrations of sodium chloride (0–60 mM). Concentrations of DNA and flavones were kept at 20 μM.

2.6 Circular dichroism (CD) studies

CD spectra were recorded in the wavelength range 200 to 700 nm using a JASCO CD spectrometer (J-1500) with a scan rate of 100 nm min^{-1} (Applied Photophysics, Leatherhead, UK). A 1 cm pathlength cell was used, and the bandwidth was kept at 1 nm. Concentrations of d(CCAATTGG)$_2$ and CT DNA were held at 20 μM and 50 μM, respectively. Flavones were added gradually in various D/N (flavones/DNA) ratios at 25 °C. The final CD spectra were the average of three scans, and the baseline was subtracted. All CD spectra were analyzed using the inbuilt software.

Open Access Article. Published on 01 September 2021. Downloaded on 4/7/2026 8:03:30 PM.
This article is licensed under a Creative Commons Attribution-NonCommercial 3.0 Unported Licence.

2.7 Differential scanning calorimetry (DSC) studies

DSC experiments were performed on a Micro Cal VP-DSC (Northampton, MA, USA). Thermal transitions from folded to the denatured state were monitored using excess heat capacity as a function of temperature. DNA samples were prepared in sodium phosphate buffer. Samples were scanned from 20 °C to 120 °C with a scan rate of 60 °C h^{-1} at constant pressure ~33 psi. A 100 μM of $d(CCAATTGG)_2$ or 300 μM free CT DNA was loaded in the sample cell and scanned to get a thermal profile for free DNA. Thermal profiles of bound forms were collected at D/N = 1. Buffer baseline was subtracted and thermograms were analyzed using the inbuilt Origin 7.1 software. Thermal profiles were fitted with a non-two-state curve fitting model.

2.8 Molecular docking studies

Molecular docking studies were done using Autodock 4.2 with MGL tools[31] to delineate the interaction between DNA and flavone compound. DNA structures $d(CCAATTGG)_2$ sequence (PDB ID:1JTL) and B-DNA dodecamer $d(CGCGAATTCGCG)_2$ (PDB ID:1BNA) were obtained from the Protein Data Bank (http://www.rcsb.org./pdb). PDB structure of 1JTL was modified to get the octamer structure. Structure data files (sdf) of flavones were converted into PDB format using Open Babel.[32] The grid boxes were prepared for octamer and dodecamer DNA with 49 × 57 × 63 and 61 × 53 × 115 number of grid points in $x \times y \times z$ directions, and with a grid spacing of 0.375 Å respectively. The Lamarckian genetic algorithm was employed for docking calculations with 100 runs. Default values were used for all other parameters. The lowest energy docked conformation was selected and PyMol software was used to visualize the docked poses.[33]

3. Result and discussion

3.1 Absorption studies

Absorption spectroscopy is a convenient and simple method to probe the binding of small molecules to DNA. Interaction of flavone compounds, baicalein, chrysin and flavone with CT DNA and an octamer promoter region sequence $d(CCAATTGG)_2$ were studied. All three flavone compounds showed absorption bands in the 200–450 nm range (ESI Fig. 1†). Band I in the 300–450 nm range is attributed to the n–π* transition in the B ring and band II in the 240–280 nm range is related to the π–π* transition in ring A.[24,34] The highest wavelength was used for analysis to minimize the overlap from DNA absorption.

3.1.1 With $d(CCAATTGG)_2$. Absorption spectra of the baicalein exhibited three bands at 222 nm, 270 nm, 336 nm (ESI Fig. 1A†). The 336 nm band, which has the least interference from the DNA absorption, was used for binding analysis. The absorbance of 336 nm decreased (hypochromism) on progressive addition of DNA, as shown in Fig. 2A, along with a slight red shift of 4 nm. An isosbestic point at 308 nm indicates the equilibrium state in the solution. The plot of absorbance with DNA concentration was shown in Fig. 2A's inset. The reciprocal of absorbance ($1/A$) plotted as a function of R represented in Fig. 2B displayed two slopes with break point around $R = 1$ suggesting a DNA : baicalein stoichiometry of 1 : 1 in the solution.[35,36]

Chrysin showed absorption bands at 208 nm, 269 nm and 328 nm (ESI Fig. 1B†). The 328 nm exhibited hypochromism when DNA was added, with no shift in the wavelength as shown in ESI Fig. 2.† Upon addition of DNA, this band was found to be overlapped with the broad band of DNA. The DNA absorbance was deducted from the observed absorbance, and the resultant absorbance after subtracting the DNA absorbance was considered for analysis and is shown in Fig. 3A. Hypochromic effect with a slight blue shift of 4 nm was observed, with absorbance reaching saturation around 24 μM. Hypochromism was highest for the first addition of DNA and after that, a gradual decrease was observed. An isosbestic point at 295 nm was observed. The reciprocal plot $1/A$ with R changed slope at $R = 1$ (Fig. 3B), indicating a stoichiometry of 1 : 1 in the solution.

Flavone showed characteristic absorbance bands around 200 nm, 252 nm and 302 nm (ESI Fig. 1C†). On successive addition of DNA, hyperchromism for the 302 nm band was observed with a significant increase in the absorbance on first addition. After that, the changes were minimal as compared to the first change. After $R = 1$, the absorbance decreased, with sporadic changes, though higher than alone flavone, as shown in Fig. 4A. An isosbestic point at 300 nm was observed (ESI

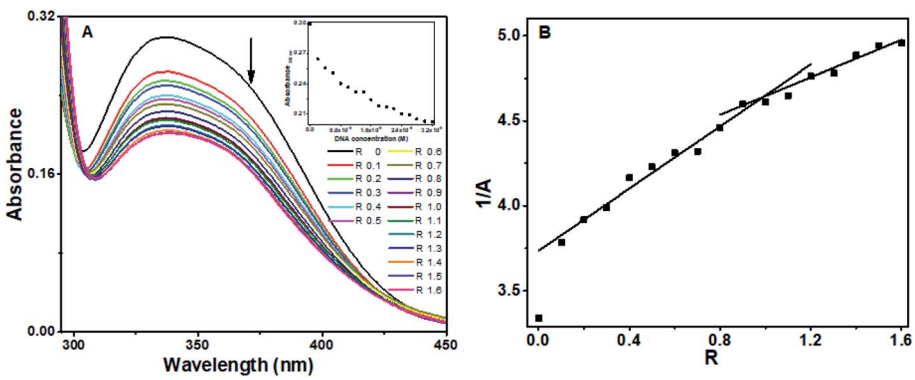

Fig. 2 Absorption spectra of (A) baicalein in the presence of different concentration of octamer DNA, inset shows plot of absorbance at 336 nm *versus* DNA concentration, (B) reciprocal plot of absorbance *versus* R.

© 2021 The Author(s). Published by the Royal Society of Chemistry

Open Access Article. Published on 01 September 2021. Downloaded on 4/7/2026 8:03:30 PM.
This article is licensed under a Creative Commons Attribution-NonCommercial 3.0 Unported Licence.

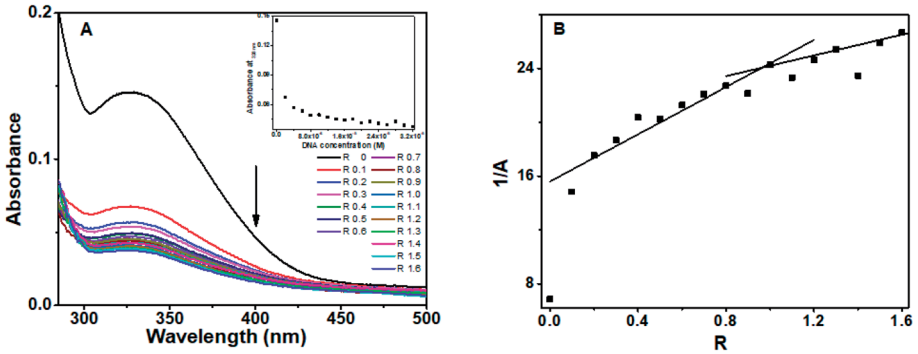

Fig. 3 Absorption spectra of (A) chrysin in the presence of different concentration of octamer DNA, inset shows plot of absorbance at 328 nm *versus* DNA concentration, (B) reciprocal plot of absorbance *versus* *R*.

Fig. 3†). The resultant spectra after the subtraction of DNA absorbance are plotted in Fig. 4A. Absorbances in the range 275–290 nm and above 320 nm were comparable with overlapping of spectra. The plot of $1/A$ with R (Fig. 4B) has two different slopes with an inflection point at $R = 0.7$, predicts the possible stoichiometry 1 : 0.7 for DNA : flavones in the solution.

Observed changes in intensity are indicative of the fluctuations in the microenvironment near the region of binding.

3.1.2 With CT DNA. The absorbance of baicalein decreased gradually (hypochromism) upon serial addition of CT DNA in different values of R, along with a redshift of 7 nm in the 336 nm band. Two isosbestic points were present in the absorption spectra, at 292 nm and 418 nm, respectively, as shown in Fig. 5A. Absorbance with DNA concentration was plotted in the inset of Fig. 5A. The reciprocal plot $1/A$ with R gives a stoichiometry for DNA–Baicalein complex in solution as 1 : 1 (Fig. 5B).

With chrysin, absorbance decreased abruptly at $R = 0.1$ without any substantial shift in the maximum absorption wavelength. After this, the decrease was small and gradual for $0.1 < R \leq 1$. The changes were minimal after $R = 1$. The absorbance was analyzed after removing the contribution from DNA as plotted in Fig. 5C. An isosbestic point observed around 288 nm, as evident in ESI Fig. 4,† which shows the absorption spectra as observed. The plot of absorbance with DNA concentration showed two different slopes (inset of Fig. 5C). An inflection point at $R = 1.1$ was obtained in the plot of $1/A$ with R, explaining a stoichiometry of 1 : 1 (Fig. 5D).

For flavone, absorbance increased sharply on the addition of DNA followed by a decrease (hypochromism) at $R \geq 0.5$. as depicted in ESI Fig 5.† An isosbestic point at 288 nm was observed. Absorbance spectra after subtraction from DNA were as shown in Fig. 5E. The plot of $1/A$ with R (Fig. 5F) has two different slopes with an inflection point at $R = 0.5$, predicts the possible stoichiometry of 1 : 0.5 for DNA : flavones in the solution.

The changes in the absorbance spectra indicate the interaction between the compounds and both octamer and CT DNA. Generally, the qualitative description in terms of hyperchromism and hypochromism with spectral shift is used to propose the mode of interaction between DNA and small molecule. Hypochromism associated with a substantial red shift is often accounted for intercalation mode of binding. In comparison, a small shift associated with hypochromism indicates partial intercalation or groove binding. Hyperchromicity, accompanied by a slight bathochromic shift, predicts electrostatic interaction.[37,38]

Therefore, baicalein and chrysin's spectral changes indicate that both are binding externally either through partial intercalation or through groove binding mode to octamer and CT DNA, evident from the hypochromicity associated with small shifts. Absence of any charge on the ligand rules out the electrostatic interaction.

With flavone, hyperchromism without any shift in wavelength until $R = 1$ hints for electrostatic or hydrogen bonding

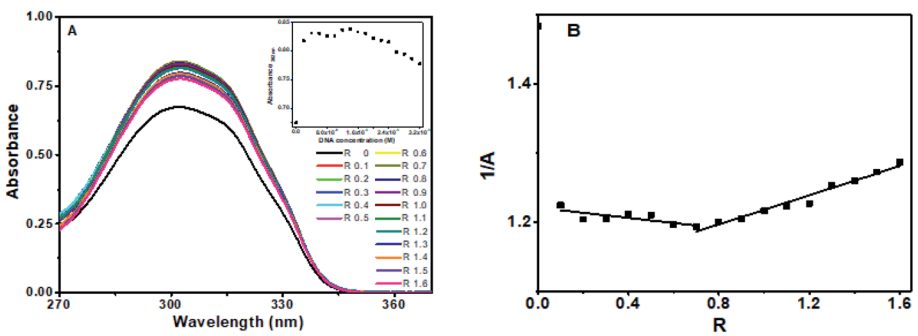

Fig. 4 Absorption spectra of (A) flavone in the presence of different concentration of octamer DNA, inset shows plot of absorbance at 302 nm *versus* DNA concentration, (B) reciprocal plot of absorbance *versus* *R*.

Open Access Article. Published on 01 September 2021. Downloaded on 4/7/2026 8:03:30 PM.
This article is licensed under a Creative Commons Attribution-NonCommercial 3.0 Unported Licence.

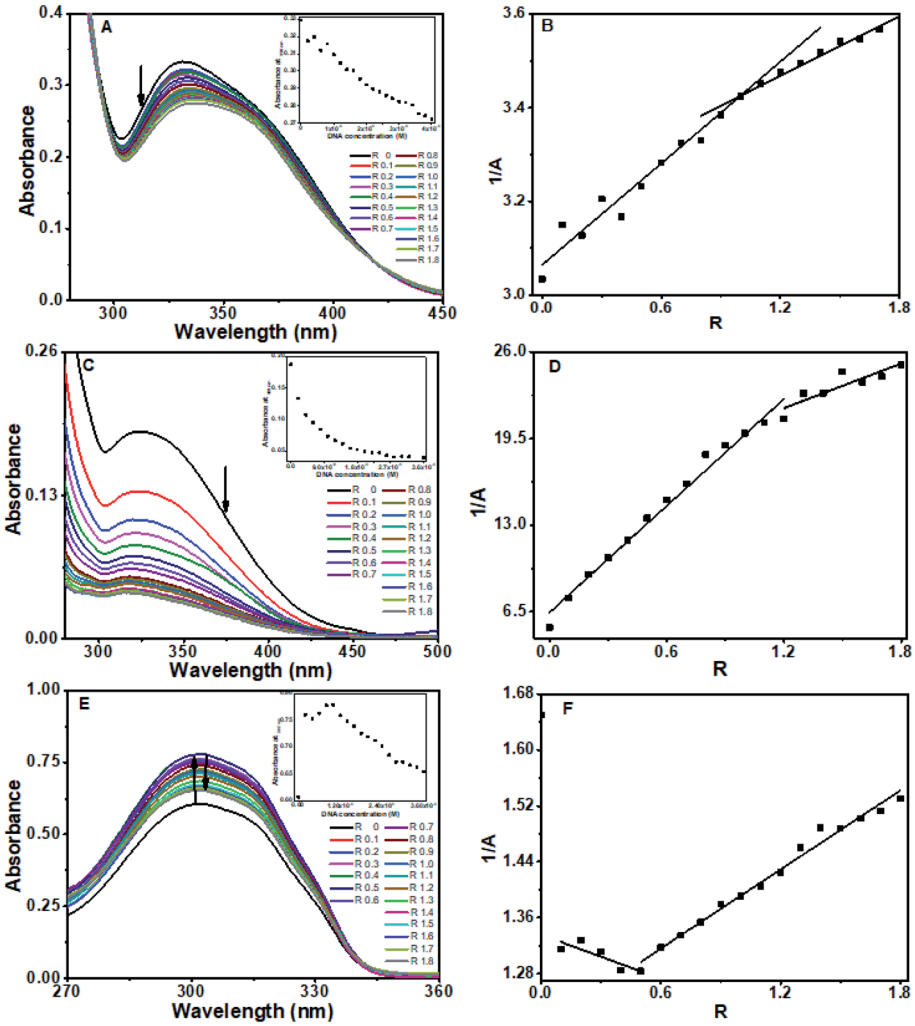

Fig. 5 Absorption spectra of (A) baicalein (C) chrysin, (E) flavone in the presence of different concentration of CT DNA. Insets show the plot of absorbance *versus* DNA concentration. Plot of 1/*A versus R* for (B) baicalein, (D) chrysin and (F) flavone respectively.

involved in the binding. The hypochromism observed for $R > 1$ and $R = 0.5$ with octamer and CT DNA, respectively, indicates that partial intercalation also plays a role. These variations usually occur when the molecule binds to DNA through partial intercalation of the aromatic rings between the base pairs.[37,39] Therefore, flavone interacts with octamer and CT DNA through two different mechanisms. The presence of isosbestic points in all cases indicates that there exists at least one equilibrium point in the solution.

Binding data were registered into Scatchard plot of *r versus* r/C_f and the isotherms with positive slope were evaluated using McGhee–von Hippel equation for cooperative binding.[40–42]

$$\frac{r}{C_f} = K_a(1-nr)\left(\frac{(2\omega+1)(1-nr)+r-R}{2(\omega-1)(1-nr)}\right)^{n-1}\left(\frac{1-(n+1)r+R}{2(1-nr)}\right)^2$$

with R equal to

$$R = \sqrt{\{[1-(n+1)r]^2 + 4\omega r(1-nr)\}}$$

where r is the number of moles of flavones bound to per mole of DNA, C_f is the concentration of free flavone, K_a is the intrinsic binding constant to an isolated binding site, n is the number of nucleotide residues covered by the ligand and ω is the cooperativity parameter.

Isotherms with initial negative slopes were fitted with binding equation in the analogous form of Scatchard equation,

$$\frac{r}{C_f} = K_a(1-nr)\left(\frac{1-nr}{1-(n-1)r}\right)^{n-1}$$

Binding constants were calculated using Scatchard plots (ESI Fig. 6†) and are quoted in Table 1. The values suggest that all three compounds bind DNA sequences with moderate to strong affinities.

3.2 Fluorescence studies

Fluorescence spectroscopy is a very sensitive technique to decipher the interaction and stoichiometry of flavones with DNA. In this technique, flavones' fluorescence properties were probed. DNA does not have intrinsic fluorescence, and flavones are weak fluorophores in aqueous solutions. Emission spectra

© 2021 The Author(s). Published by the Royal Society of Chemistry

Open Access Article. Published on 01 September 2021. Downloaded on 4/7/2026 8:03:30 PM.
This article is licensed under a Creative Commons Attribution-NonCommercial 3.0 Unported Licence.

Table 1 Binding constants of flavones in the presence of d(CCAATTGG)$_2$ and CT DNA

	Binding constant d(CCAATTGG)$_2$ (M^{-1})				Binding constant CT DNA (M^{-1})			
	From absorbance		From fluorescence,		From absorbance		From fluorescence,	
	K_b (M^{-1})	N	K_b (M^{-1})	n	K_b (M^{-1})	n	K_b (M^{-1})	n
Baicalein	2.24×10^5	2.5	3.4×10^3	2.83	4.65×10^5	1.17	4.47×10^3	2.9
Chrysin	1.21×10^5	2.65	9.07×10^3	2.9	9.03×10^5	2.62	3.03×10^5	4
Flavone	8.42×10^5	1.05	9.47×10^3	3.78	2.18×10^5	1.07	—	—

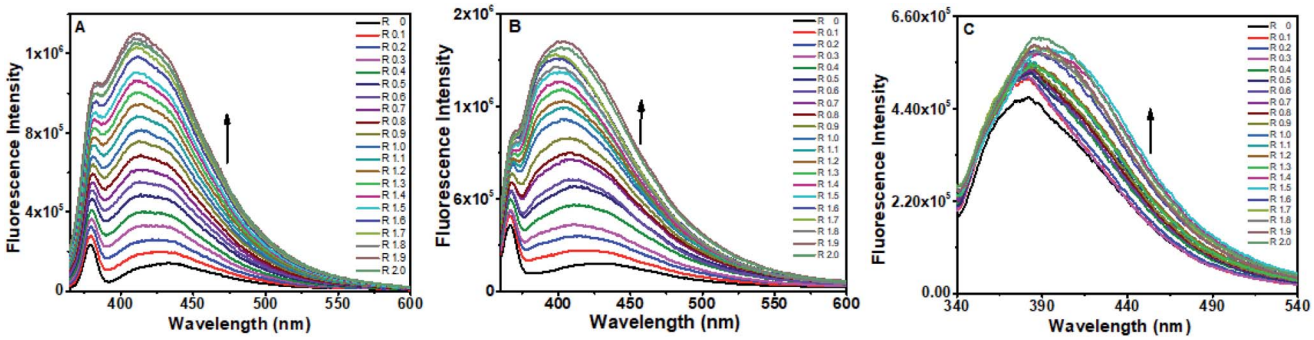

Fig. 6 Fluorescence spectra of (A) baicalein, (B) chrysin and (C) flavone with different concentration of octamer DNA.

of baicalein, chrysin and flavone show broad bands around 436 nm, 426 nm and 381 nm when excited at 336 nm, 326 nm and 302 nm respectively (ESI Fig. 7 A–C†).

The emission spectra of the three compounds were recorded at different pH values (pH = 2 to 10). At lower pH the emission intensities were lower (pH 2 and 4) and at higher pH (pH 9 and 10) intensity increased. At pH 5, 6, 7 emission intensities were almost same. A minute blue shift and red shift were observed at low and high pH conditions respectively with respect to pH 7. Flavone did not show significant changes with pH. The changes in spectra can be due to the deprotonation of the compounds and for flavone no significant changes observed due to the absence of OH groups. Spectra at different pH were shown in ESI Fig. 8 A–C.† For pH 5 to 7, fluorescence intensity did not change notably for all three compounds. All experiments were performed at pH 7.

3.2.1 With d(CCAATTGG)$_2$. Enhancement of fluorescence intensities of baicalein, chrysin and flavone was observed upon addition of d(CCAATTGG)$_2$ DNA, which indicate the binding of flavones molecules with DNA. The fluorescence from baicalein and chrysin were increased, upon addition of d(CCAATTGG)$_2$ in different R values with blue shifts of ~20 nm and ~30 nm respectively (Fig. 6A and B). The significant changes in fluorescence intensity indicated a strong association with d(CCAATTGG)$_2$. With flavone, a slight increase in fluorescence intensity with a redshift of ~8 nm was observed (Fig. 6C). An isoemissive region of 348 nm to 357 nm was obtained in this case. Fluorescence increased by 690%, 664% and 27% for baicalein, chrysin and flavone, respectively. Reciprocal of fluorescence intensity (1/F) plot against R for octamer-DNA confirms that a 1 : 0.6 stoichiometric ratio of baicalein : DNA as well as chrysin : DNA complexes present in their respective solutions

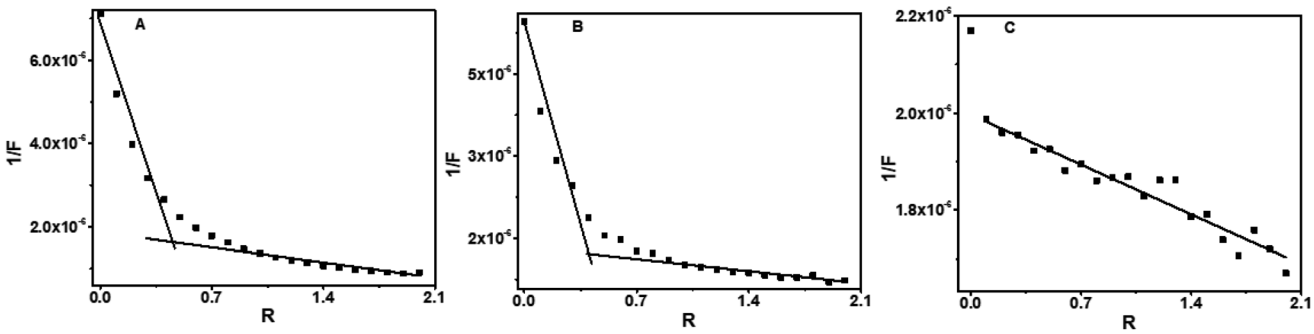

Fig. 7 Plot of 1/F *versus* R for baicalein (436 nm) (A), chrysin (426 nm) (B) and flavone (381 nm) (C) with octamer DNA.

Open Access Article. Published on 01 September 2021. Downloaded on 4/7/2026 8:03:30 PM.
This article is licensed under a Creative Commons Attribution-NonCommercial 3.0 Unported Licence.

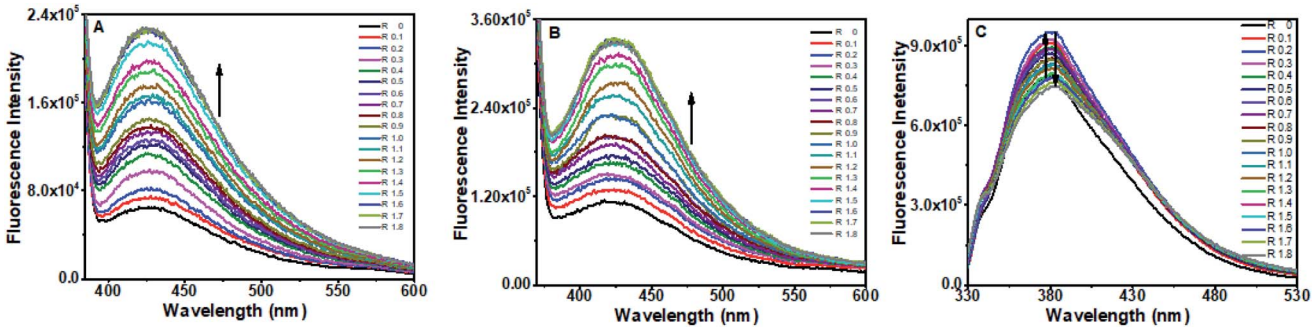

Fig. 8 Fluorescence spectra of (A) baicalein (B) chrysin and (C) flavone with different concentration of CT DNA.

(Fig. 7A and B), whereas many inflection points were observed in the case of flavone (Fig. 7C). The fluctuations of points in flavone's plot indicate heterogeneous binding of flavone.

Binding constants (K_b) were calculated McGhee–von Hippel equation as described in Section 3.1 and the plots were displayed in ESI Fig. 9 A–C,† and values are given in Table 1.

3.2.2 With CT DNA. Emission intensities of baicalein and chrysin were gradually increased upon the addition of different CT DNA concentrations without any change in the emission wavelength, as shown in Fig. 8A and B. There was no further increase in fluorescence intensity upon addition of CT DNA after $R = 1.6$ ([DNA] = 32 μM) for baicalein and 1.2 ([DNA] = 24 μM) for chrysin. Fluorescence increased by 300% for baicalein and 247% for chrysin. In comparison, only a moderate change in the fluorescence intensity was observed for flavone when CT DNA was added (Fig. 8C). The fluorescence intensity increased for $R = 0.1$ and 0.2 and decreased after that, though the intensity is higher than alone flavone till $R = 1.6$. Intensity fell below alone intensity after $R = 1.6$. No further significant change was observed around $R = 1.6$.

The $1/F$ *vs.* R plot shows inflection points at 0.45 and 0.6 respectively for baicalein and chrysin. Hence the possible stoichiometries that exist are 1 : 0.45 and 1 : 0.6 for these two compounds (Fig. 9 A–C). The plot was linear with fluctuations in the data points for flavone, indicating the possibility of multi-stoichiometric complexes in the solution.

Fluorescence spectral variations indicate the mode of interaction and changes in the local environment of the fluorophores. In DNA–small molecule interaction, a large blue shift associated with an increase in the fluorescence intensity demonstrates the groove mode of binding. In contrast, a redshift with an enhancement in intensity is related to the intercalation mode of binding.[43]

In this study, the blue shift in emission wavelengths of baicalein and chrysin and a significant enhancement of the intensity when complexed with octamer DNA suggest that these two molecules are in a nonpolar environment than when it is present in aqueous solution in the free state.

For flavone, the bathochromic shift in wavelength and the increment in intensity are minimal. These spectral features indicate partial intercalation or an external binding of flavone with DNA base pairs. The intensity variations (increase followed by decrease) suggest that electrostatic interaction and hydrogen bonding may also be involved in the binding between the two.

Baicalein fluorescence increased by more than an order, while chrysin fluorescence increased three times without any shift in the emission wavelength when complexed with CT DNA. Hence intercalation of these molecules into CT DNA is ruled out. The observed changes indicate that the two molecules are now in a more hydrophobic environment and might have intercalated. For flavone, the intensity first increased, then decreased. These changes indicate external binding or partial intercalation along with electrostatic interaction and hydrogen bonding.[44,45]

Therefore, it can be deduced that baicalein and chrysin interact with both octamer and CT DNA through partial intercalation. At the same time, flavone might have partially

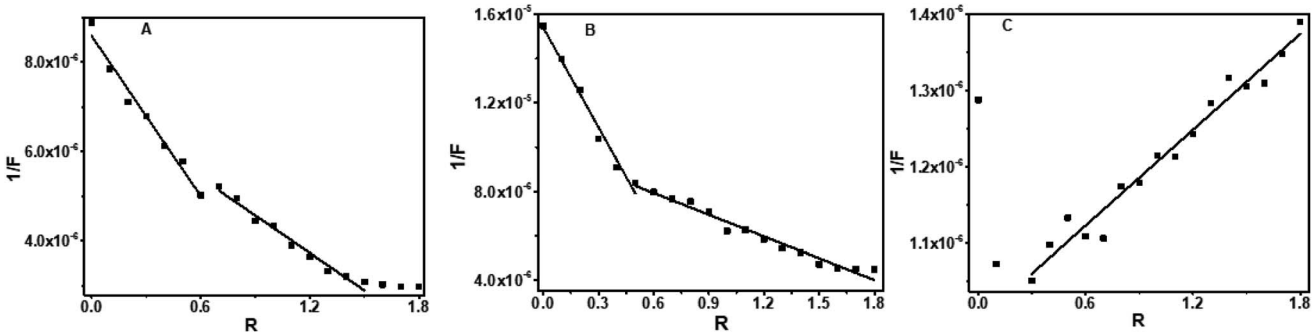

Fig. 9 Plot of $1/F$ *versus* R for baicalein (436 nm) (A), chrysin (426 nm) (B) and flavone (381 nm) (C) with CT DNA.

© 2021 The Author(s). Published by the Royal Society of Chemistry

Open Access Article. Published on 01 September 2021. Downloaded on 4/7/2026 8:03:30 PM.
This article is licensed under a Creative Commons Attribution-NonCommercial 3.0 Unported Licence.

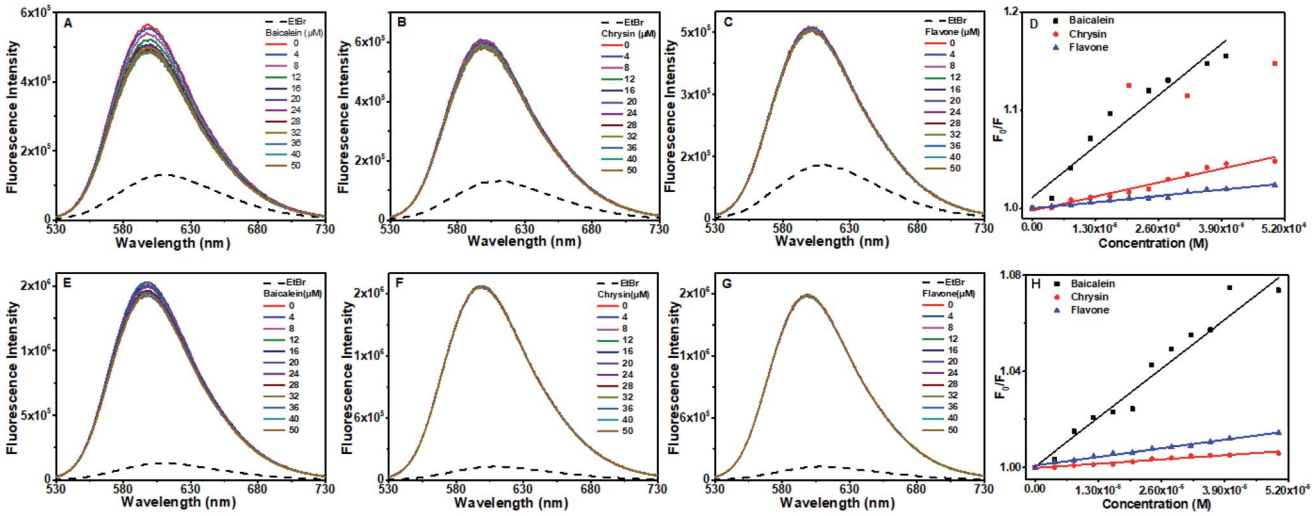

Fig. 10 Fluorescence quenching spectra of octamer DNA–EtBr (A–D) and CT DNA–EtBr (E–H) upon addition of baicalein, chrysin and flavone (0–50 μm) respectively and Stern–Volmer quenching plot of flavones. The DNA–EtBr complex was excited at 476 nm and emission spectra were recorded from 500 to 750 nm.

intercalated or externally bound to the DNA. Similar observations are obtained from the absorption data.

Binding constants (K_b) were calculated McGhee–von Hippel equation as described in Section 3.1 and the plots were displayed in ESI Fig. 9† and values are given in Table 1. Scatchard plot was not done in the case of flavone as there was increase and decrease of fluorescence intensity while titration, leading to scattered data points. Similar values for binding constants were reported for flavones and other small molecules compounds in literature.[24,46,47]

3.3 Displacement assay

Many DNA binding dyes can be employed to decipher the mode of DNA–ligand interaction. In competitive displacement assay, the ligand that displaces the dye bound to DNA interacts in the same manner as that of the displaced dye. Variations in the DNA–dye system's emission profile, on addition of the ligand, can give hints about the mode of binding.[48,49]

3.3.1 Ethidium bromide (EtBr) displacement. Ethidium bromide (EtBr), a weak fluorophore in an aqueous solvent, fluoresce intensely when binds to DNA in the intercalative mode of binding. In EtBr displacement assay, any molecule that binds intercalatively to DNA displaces the dye and decreases dye's fluorescence (quenching). The extent of the fluorescence quenching will give knowledge on the extent of intercalation by the ligand molecule.

Fig. 10A–C displays the emission profiles of the octamer DNA–EtBr system along with the addition of different concentrations of baicalein, chrysin and flavone, respectively. The emission intensity of EtBr changed slightly with baicalein whereas chrysin and flavone no significant changes were observed (till 50 μM), implicating that these compounds are not intercalated completely in the DNA helix and were not able to displace EtBr from its intercalated position. Stern–Volmer quenching plots are represented in Fig. 10D.

With the CT DNA–EtBr system, the spectral change and Stern–Volmer plots with various concentrations of flavone compounds are given in Fig. 10E–G. As evident in the figure, the CT DNA–EtBr fluorescence did not get affected by the addition of the compounds. Hence, it indicates that all three compounds could not displace EtBr completely. Quenching constants are tabulated in Table 2.

3.3.2 Hoechst displacement. Hoechst 33258 displacement assay was performed to probe the minor groove binding of the compounds. Hoechst 33258 is a DNA AT region binding dye that is a weak fluorophore in aqueous solutions. However, in the presence of DNA, its emission increases substantially.[50,51] Any molecule that binds to the AT region of DNA will displace Hoechst from its position, resulting in the quenching of the DNA–Hoechst system's fluorescence intensity. Fig. 11A–C shows the changes in the octamer DNA–Hoechst system's fluorescence spectra upon adding the three compounds. With baicalein and chrysin, quenching in the emission

Table 2 Stern–Volmer quenching constants (K_{sv}) values of Hoechst and EtBr with CT DNA and d(CCAATTGG)$_2$ upon addition of flavones

	d(CCAATTGG)$_2$		CT DNA	
Compound	K_{sv} (10^3 M^{-1}), with EtBr	K_{sv} (10^3 M^{-1}), with Hoechst	K_{sv} (10^3 M^{-1}), with EtBr	K_{sv} (10^3 M^{-1}), with Hoechst
Baicalein	3.20	4.21	1.57	7.95
Chrysin	1.08	6.47	0.13	9.24
Flavone	0.48	1.35	0.27	5.93

© 2021 The Author(s). Published by the Royal Society of Chemistry

Open Access Article. Published on 01 September 2021. Downloaded on 4/7/2026 8:03:30 PM.
This article is licensed under a Creative Commons Attribution-NonCommercial 3.0 Unported Licence.

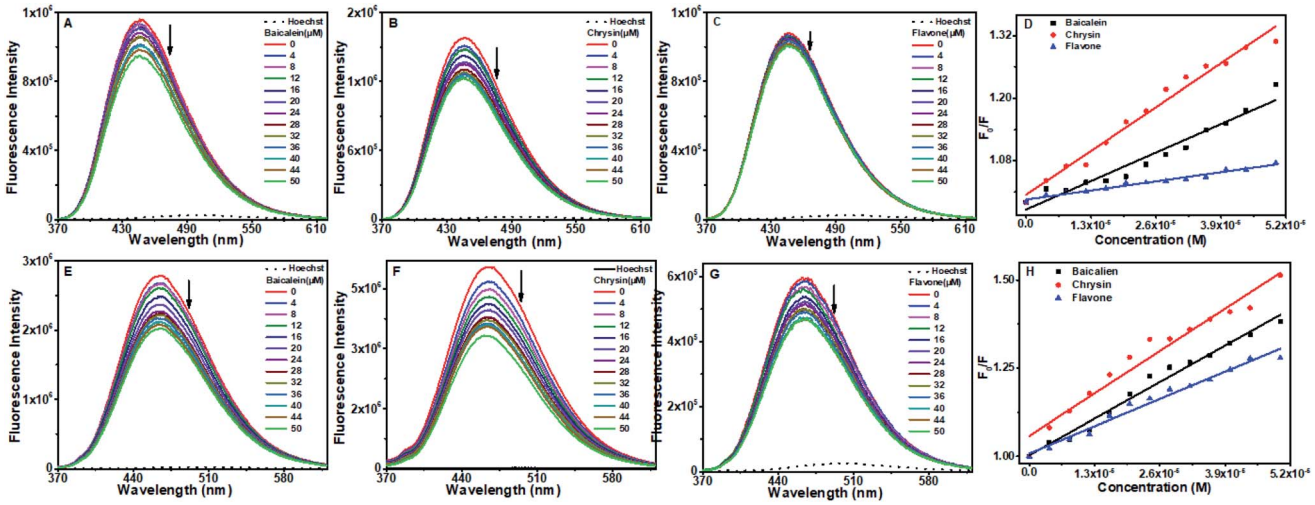

Fig. 11 Fluorescence quenching spectra of octamer DNA-Hoechst (A–D) and CT DNA-Hoechst (E–H) upon addition of baicalein, chrysin and flavone (0–50 μm) respectively and Stern–Volmer quenching plot of flavones. DNA–Hoechst complex was excited at 343 nm and emission spectra were recorded from 350 to 650 nm.

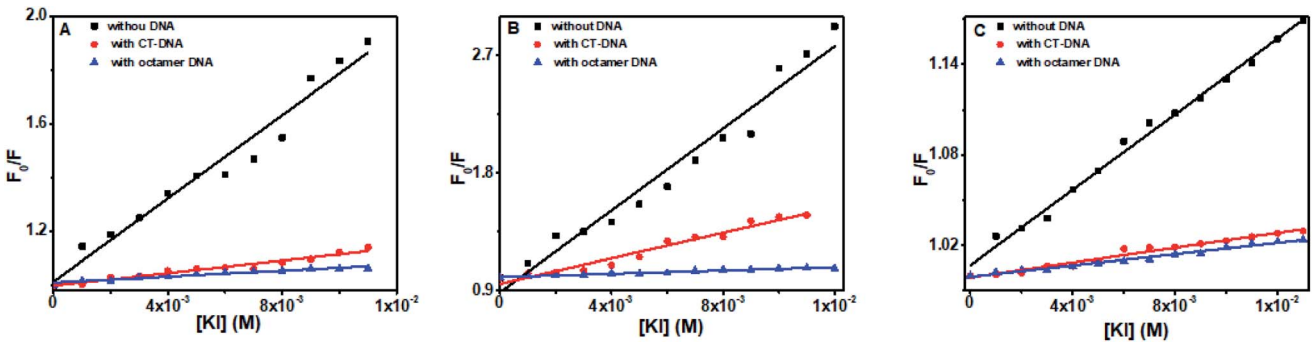

Fig. 12 Stern–Volmer quenching plot of (A) baicalein, (B) chrysin and (C) flavone in the absence and presence of CT-DNA and d(CCAATTGG)$_2$ respectively upon successive addition of KI.

intensity was observed, while no change was observed for flavone. These observations indicate that baicalein and chrysin displace Hoechst from its position and bind to octamer DNA near the AT region. Since flavone did not produce any change in the fluorescence intensity, it is not displacing Hoechst from its bound position. Therefore, it can be presumed that flavone is not binding near the minor groove.

Fluorescence from the CT DNA–Hoechst system got quenched increasingly upon the progressive addition of all three flavone compounds indicating that they could displace Hoechst from its bound place. Quenching in the presence of chrysin was more, and the least quenching was by flavone.

EtBr displacement data suggest that the flavone compounds are not completely intercalated and signals for partial intercalation. In Hoechst dye displacement, the intensity variations suggest that the compounds are able to displace it to some extent indicating that they are bound near the AT region. Hoechst dye can bind to the unwound regions of DNA at higher concentration. Therefore this result cannot confirm its minor groove binding. Correlation with other data reported therefore indicate for a partial intercalation.

3.4 Potassium iodide (KI) quenching studies

Fluorescence quenching is a supportive method to investigate the binding mode of small molecules to double-helix DNA. DNA has polyanionic phosphate backbones, which can repel an anionic quencher. When a molecule is intercalated into the DNA, it will not be affected by the external anionic quencher. In

Table 3 Stern–Volmer quenching constants (K_{sv}) values of flavones in the absence and presence of CT-DNA and d(CCAATTGG)$_2$ by increasing the concentration of KI

Flavones	Without DNA (M^{-1})	With CT-DNA (M^{-1})	With d(CCAATTGG)$_2$ (M^{-1})
Baicalein	76.58	11.67	4.94
Chrysin	161.99	52.28	6.25
Flavone	5.26	2.76	2.26

© 2021 The Author(s). Published by the Royal Society of Chemistry

Open Access Article. Published on 01 September 2021. Downloaded on 4/7/2026 8:03:30 PM.
This article is licensed under a Creative Commons Attribution-NonCommercial 3.0 Unported Licence.

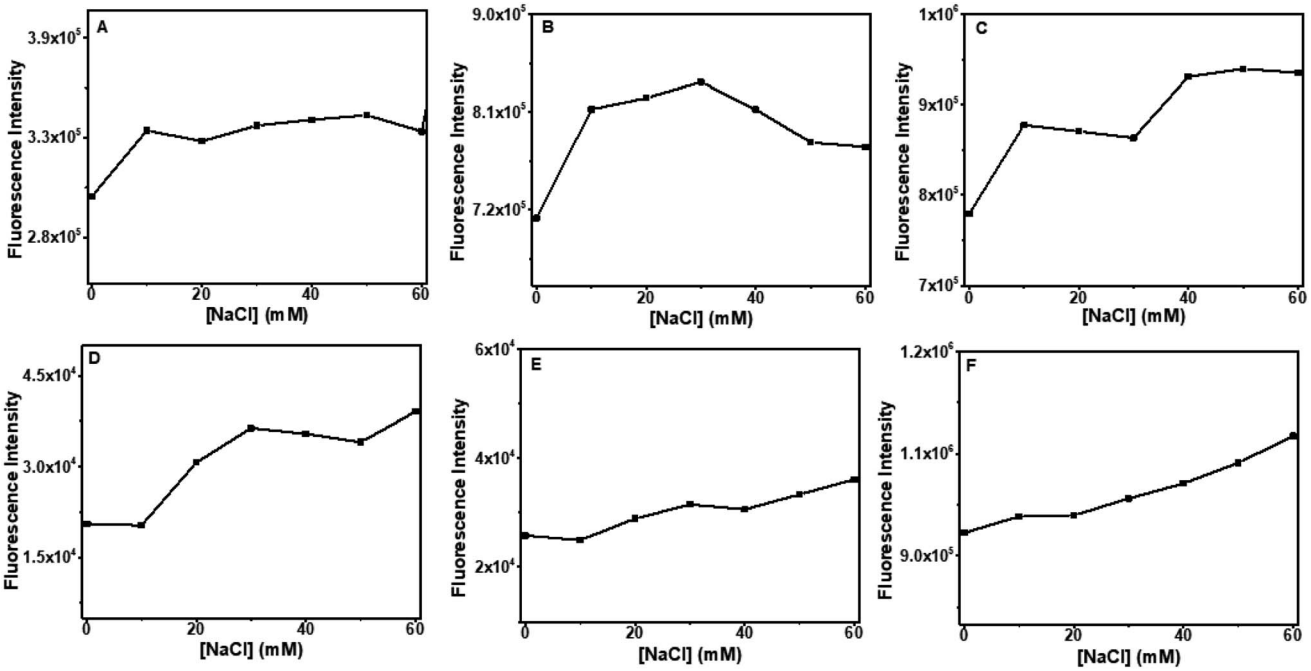

Fig. 13 Effect of ionic strength, maximum emission intensities of DNA–flavones was plotted against the increasing concentration of NaCl. The concentration of flavones and DNA were kept at 20 μM. Plots (A–C) baicalein, chrysin and flavone with octamer DNA, and plots (D–F) baicalein, chrysin and flavone with CT-DNA respectively.

contrast, partially intercalated or groove binding molecules will be less protected from the quencher[52,53] and can get quenched to a certain extent.

Flavones in solution was effectively quenched by KI (Fig. 12). In CT DNA and octamer DNA's presence, fluorescence intensities of baicalein, chrysin, and flavone were decreased minutely with the increasing amount of KI. However, the scale of quenching was very less. Stern–Volmer quenching constants (K_{sv}) were calculated, and the magnitude of K_{sv} in the presence of both DNA are given in Table 3. The K_{sv} values in the presence of DNA were very small compared to the value when they were in free form. The data suggest that baicalein and chrysin are quenched minutely, still not completely accessible to KI when they complex with DNA. These changes indicate that the compounds are in hydrophobic pockets and are not completely accessible to KI when bound to DNA. All the three flavones' fluorescence got quenched more in the presence of CT DNA than compared to the octamer sequence.

3.5 Effect of ionic strength

The effects of ionic strength in the formation of DNA–flavones complexes were analyzed using NaCl titration experiments. Titration of the electrolyte NaCl to the DNA–flavone bound solution can weaken the electrostatic interaction between the flavones and DNA. This can lead to the ejection of the compound from its position.[54,55]

Changes in the fluorescence spectra of flavones–DNA system with increasing concentrations of NaCl (0–60 mM) were studied. It is observed that the fluorescence intensity of the compounds increased slightly on the addition of NaCl, as displayed in Fig. 13. No substantial variations were observed in the emission of DNA–baicalein and DNA–chrysin complexes after adding

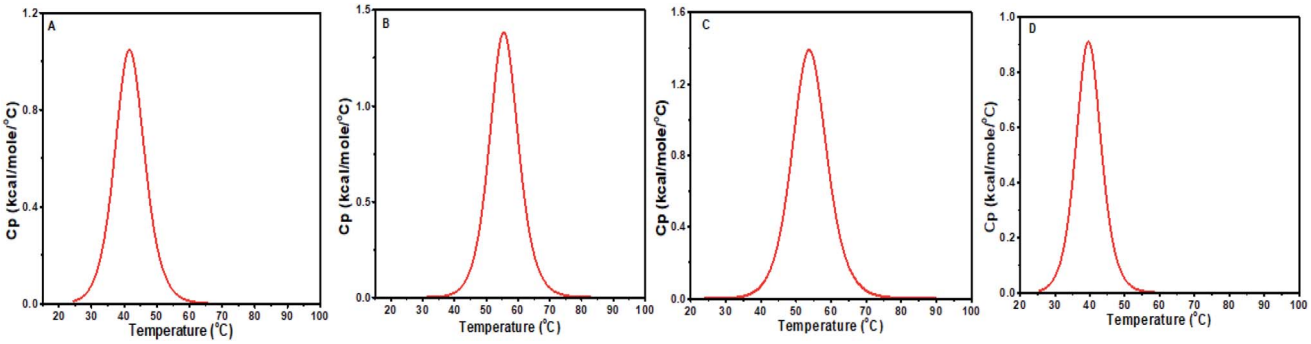

Fig. 14 DSC thermograms showing excess heat capacity as the function of temperature for (A) free d(CCAATTGG)$_2$ and complex at D/N = 1.0, with (B) baicalein, (C) chrysin, and (D) flavone.

Open Access Article. Published on 01 September 2021. Downloaded on 4/7/2026 8:03:30 PM.
This article is licensed under a Creative Commons Attribution-NonCommercial 3.0 Unported Licence.

Table 4 Thermodynamic properties of d(CCAATTGG)$_2$ DNA sequence in the presence of flavones

Sample	T_m (°C)	ΔH (kcal mol^{-1})	ΔH_V (kcal mol^{-1})	m ($\Delta H_V/\Delta H$)	ΔT_m (°C)
d(CCAATTGG)$_2$	41.73	12.65	65.17	5.15	—
d(CCAATTGG)$_2$ baicalein1 : 1	55.61	16.58	71.67	4.32	13.88
d(CCAATTGG)$_2$ chrysin1 : 1	53.87	18.17	65.00	3.57	12.14
d(CCAATTGG)$_2$ flavone1 : 1	39.66	8.72	81.28	9.32	−2.07

a sufficient amount of the salt. All the compounds have negligible fluorescence in the aqueous buffer than their DNA-bound form (see Fluorescence section). Therefore, the slight increase in the fluorescence tells that they are very much in the bound state and are well protected from the aqueous medium. This means that electrostatic interaction has only a small role in binding baicalein and chrysin with CT DNA and the octamer DNA sequences.

In contrast, the emission intensity increased by an apparent magnitude for the DNA–flavone system. The helix now gets tightened due to the electrostatic interaction between the negatively charged phosphate backbone and Na^+ ions. Then the flavone is placed well into the hydrophobic region where it is protected from the cations. Since flavone is a small compact molecule, it might have got placed deep into the hydrophobic region and resulted in a slightly higher fluorescence.

4. Differential scanning calorimetry (DSC) studies

DSC is used to investigate the thermally induced structural transitions of DNA and its complex with a small molecule. The binding of baicalein, chrysin and flavone to both d(CCAATTGG)$_2$ sequence and CT DNA were examined from DSC results using the shift in melting temperature T_m (ΔT_m). DSC profiles were fitted with a non-two state model to obtain the best fit (Fig. 14). Table 4 reports the observed values of the heat enthalpies and T_m. Free octamer DNA was fitted with a single peak showing melting transition centered at $T_m = 41.73$ °C. The binding of baicalein and chrysin shifted T_m by 13.8 °C and 12.1 °C, which agrees for strong binding of these flavones with DNA. At the same time, T_m decreased by 2 °C for flavone–DNA complex, which implies its weak affinity to the DNA. Similar reduction or no change in T_m was reported for different flavones by Vitorino *et al.*[13] The calorimetric enthalpy (ΔH) increased compared to alone DNA in the case of baicalein–DNA and chrysin–DNA complexes. These two compounds with more OH groups are binding more strongly as compared to flavone in which OH groups are replaced by H atoms (Fig. 1). These changes indicate that the structural changes in these three flavones are responsible for their differential binding.

CT DNA DSC profile exhibited a small peak followed by a broad peak, shown in Fig. 15. This feature may be due to more than two melting pathways or independent melting pathways from the single stranded and double stranded composition of CT DNA. The curve was fitted with three peaks to get the best fit. The second (T_{m2}) and third (T_{m3}) peaks were considered for analysis as they are closer to the melting temperature of CT DNA provided by the manufacturer. The first peak also showed a significant shift upon interacting with the compounds. As shown in Table 5, $\Delta T_{m2} = 6.95$ °C and 2.8 °C and $\Delta T_{m3} = 7.19$ °C and 5.22 °C for baicalein and chrysin, respectively, while ΔT_{m1} showed large deviation from the alone DNA value. The changes indicate a strong binding between CT DNA and molecules. For flavone, the shifts are small (~0.5 °C) and hence represent low stability of its complex with CT DNA. The ratio of van't Hoff enthalpy to calorimetric enthalpy ($\Delta H_V/\Delta H = m$) gives the average size of the simultaneous melting region of DNA. In a two-state behavior, $m = 1$ indicating that the DNA is directly converted to its denatured form. A deviation from this suggests a multi-state process where many intermediate states will be formed during the denaturing process.[56,57]

Therefore, DSC data ascertained that baicalein and chrysin interact strongly with both DNAs forming stable complexes with a higher affinity for the octamer DNA sequence. Flavone exhibited a lower affinity with both DNA sequences and the

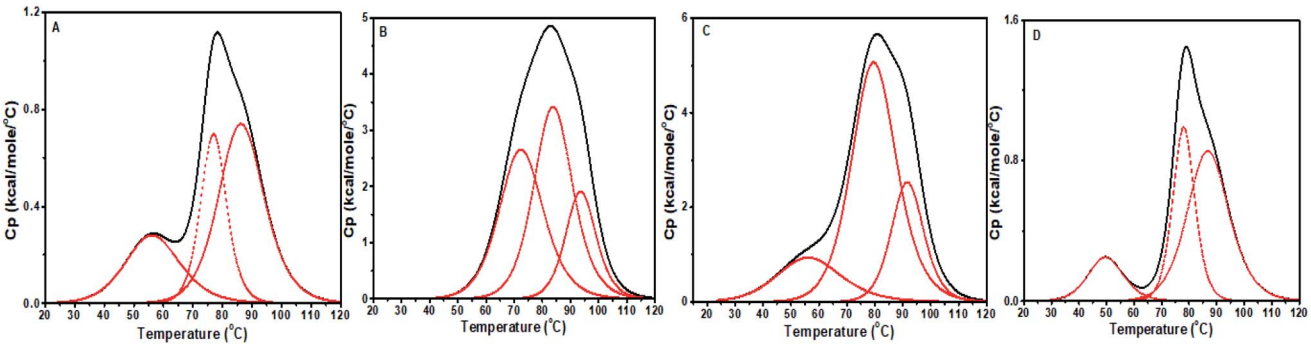

Fig. 15 DSC thermograms showing excess heat capacity as the function of temperature for (A) free CT DNA, and complex at D/N 1.0, with (B) baicalein, (C) chrysin, and (D) flavone.

© 2021 The Author(s). Published by the Royal Society of Chemistry

Open Access Article. Published on 01 September 2021. Downloaded on 4/7/2026 8:03:30 PM.
This article is licensed under a Creative Commons Attribution-NonCommercial 3.0 Unported Licence.

Table 5 Thermodynamic parameters of CT DNA in the presence of flavones

Sample	T_{m1} (°C)	ΔH_1 (kcal mol^{-1})	ΔH_{V1} (kcal mol^{-1})	$\Delta H_{V1}/\Delta H_1$	T_{m2} (°C)	ΔH_2 (kcal mol^{-1})	ΔH_{V2} (kcal mol^{-1})	m ($\Delta H_{V2}/\Delta H_2$)	T_{m3} (°C)	ΔH_3 (kcal mol^{-1})	ΔH_{V3} (kcal mol^{-1})	ΔT_{m2} (°C)	ΔT_{m3} (°C)
CT DNA	56.60	6.86	35.26	5.13	77.05	8.16	83.30	10.2	86.54	15.26	49.83	—	—
CT DNA–baicalein 1 : 1	72.71	55.36	45.54	0.82	84.0	52.91	55.03	1.04	93.73	27.53	74.17	6.5	7.19
CT DNA–chrysin1 : 1	56.79	28.43	28.42	0.99	79.88	108.0	46.36	0.43	91.76	38.94	68.83	2.83	5.22
CT-DNA–flavone 1 : 1	49.80	4.25	48.6	11.4	78.10	10.46	92.95	8.8	87.07	17.27	50.98	1.05	0.53

complexes were less stable. The higher ΔT_m values for baicalein and chrysin indicates the intercalation mode of binding.

5. Circular dichroism (CD) studies

CD spectroscopic technique is helpful to monitor the conformational changes of DNA in different conditions. The observed CD spectra of d(CCAATTGG)$_2$ and CT DNA exhibited characteristic positive bands around 273 nm and 279 nm, respectively, due to base stacking and negative band around 240 nm and 245 nm due to the helicity of the DNA, the signature peaks of DNA in the right-handed B form.[58,59] The changes in the CD spectra of DNA on the addition of flavone compounds were examined. The differences can be accounted for the corresponding alterations in the DNA structure.[60,61] The three flavones under study did not show any significant signal in their CD spectra. The changes observed when flavone compounds were incubated with both the DNA, were depicted in ESI Fig. 10.† The intensities of the bands were changed without any induced signal.

5.1 With octamer

The CD values of 240 nm and 273 nm bands of octamer DNA were decreased gradually when complexed with increasing concentrations of baicalein. The 240 nm band decreased by 88% at D/N = 2 without any significant shift while the 273 nm band decreased by 22% at D/N = 2 respectively with a red shift of ~5 nm. With chrysin, the 240 nm band reduced by 16% at D/N = 2. The 273 nm band gradually reduced till D/N = 1 (27%) and after that the CD value increased slightly. No shift in wavelength was observed. Whereas for flavone, CD values decreased by 54% and 50% for negative and positive bands respectively without any shift. An isodichroic point around 259 nm indicates the existence of one major complex in the solution.

5.2 With CT DNA

Similar nature in the CD spectra were observed with CT DNA. With baicalein, the CD values of the positive band at 279 nm decreased by 65% at D/N = 2 with a red shift of 14 nm. The negative band at 245 nm decreased by 80% at D/N = 2 without any shift. With chrysin, there was only a slight decrease in the CD bands without any shift. Complexation of flavone with CT DNA resulted in the reduction in intensities of the CD bands. There was a blue shift of 7 nm with a decrease in intensity of 64% at D/N 2 respectively for 279 nm band while 245 nm band decreased by 61% at D/N = 2 along with a blue shift of ~4 nm. The intensity changes in the CD bands observed indicate the changes induced in the DNA conformation when flavones bound to both the DNA.

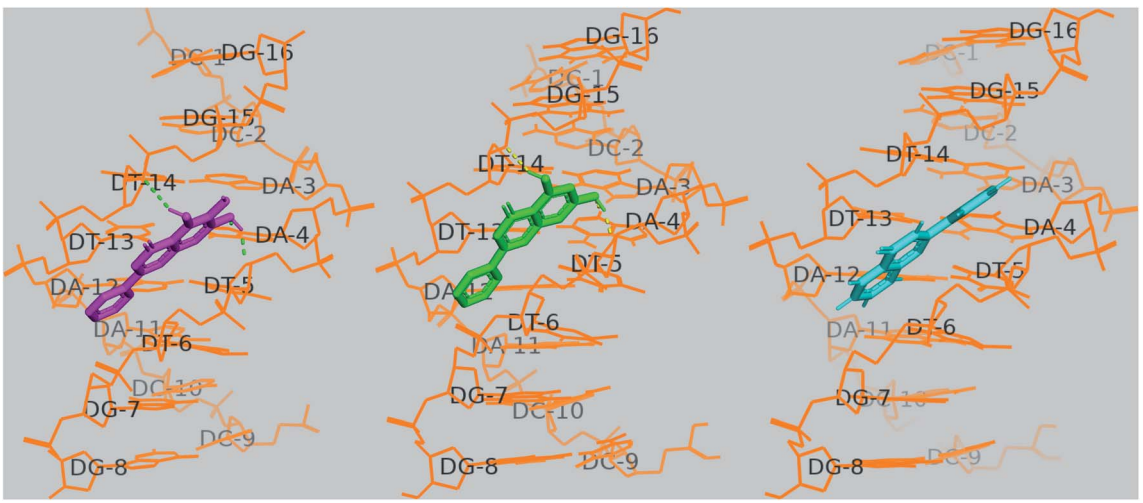

Fig. 16 Docked poses of baicalein (magenta), chrysin (green) and flavone (cyan) with octamer DNA. Hydrogen bonds are shown as dashed lines.

Open Access Article. Published on 01 September 2021. Downloaded on 4/7/2026 8:03:30 PM.
This article is licensed under a Creative Commons Attribution-NonCommercial 3.0 Unported Licence.

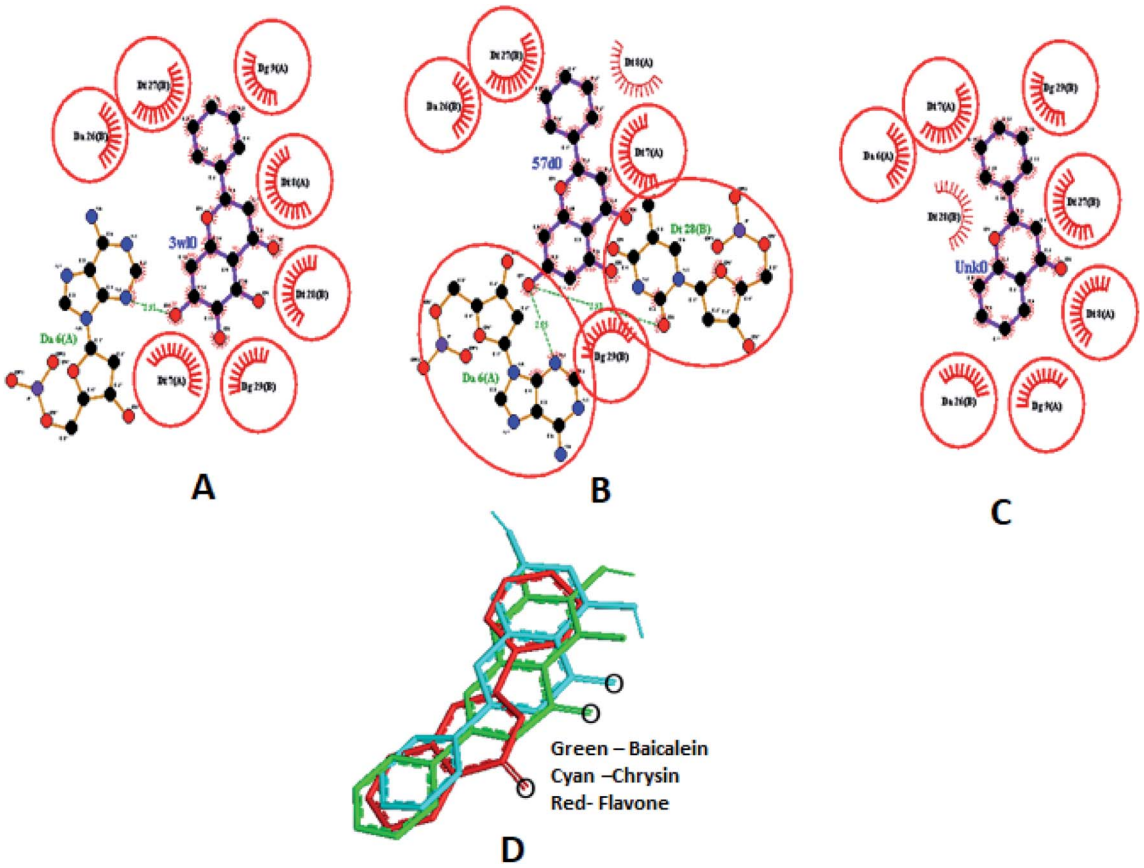

Fig. 17 Ligplot showing the interactions of baicalein (3w10) (A), chrysin (57d0) (B) and flavone (Unk0) (C) with octamer DNA. Hydrophobic interactions are shown as red lines, hydrogen bond interactions are in green, red circles and ellipses shows the equivalent sites among three complexes, thick red bonds represent equivalent residues involved in hydrophobic interaction. Docked poses of baicalein, chrysin and flavone superimposed (D).

The data shows that the changes were notably high with baicalein followed by flavone and least for chrysin. The changes in both bands indicate perturbation in the helicity as well as the stacking interaction of DNA causing a major conformational change in DNA. Decrease of the CD bands indicates changes in the helicity of DNA when it binds with a ligand and generally correlated to intercalation or groove binding of the ligand. Decrease in intensities of both bands is observed in the case of intercalation.[62,63] Therefore, the CD changes for baicalein and flavone hints at the intercalation of them. Absence of any induced band hints that the molecules oriented not parallel to the nucleotide bases, but in a tilted fashion.[64] The changes observed therefore predict that baicalein and flavone might have intercalated partially or in a tilted fashion. The dye displacement data supports this response.

Chrysin on the other hand did not exhibited any significant changes in the CD bands. The fluctuations in the baseline region above 300 nm is more for chrysin. These fluctuations without any noticeable changes hints for an intercalative mode of binding.[64] The isodichroic regions (248 nm to 259 nm; 286 nm to 294 nm) observed indicate a strong complex formation through a single mode of binding. Absorbance and fluorescence intensities of all three compounds showed linearity with concentration ruling out the aggregation effects.

6. Molecular docking studies

Molecular docking is one of the most attractive techniques to understand the binding mechanism of small ligands with double-helical DNA in drug designing and elucidate the location of binding sites in target-specific interactions of the DNA. In this study, the three flavone compounds were docked with two duplex DNA sequences; $d(CCAATTGG)_2$ (PBD ID:1JTL) and $d(CGCGAATTCGCG)_2$ dodecamer (PDB ID:1BNA). Molecular docking provided the energetically favorable docked conformations and predicted first docked poses with the lowest energy were selected for analysis, out of hundred runs.

6.1 With octamer sequence $d(CCAATTGG)_2$

The docking results showed that the three flavones are bound to the central region of the DNA helix with a proximity to the AATT segment. With the octamer sequence $d(CCAATTGG)_2$, baicalein and chrysin formed three hydrogen bonds each; with adenine (NH of A4; 1.9 Å), with the sugar-phosphate backbone of thymine bases (O4′ of T5, 2 Å; O3′ of T14, 2.5 Å). Binding energies for baicalein, chrysin

© 2021 The Author(s). Published by the Royal Society of Chemistry

Open Access Article. Published on 01 September 2021. Downloaded on 4/7/2026 8:03:30 PM.
This article is licensed under a Creative Commons Attribution-NonCommercial 3.0 Unported Licence.

and flavone were −8.28 kcal mol^{-1}, −8.74 kcal mol^{-1}, −8.46 kcal mol^{-1}, respectively. The H bond lengths are within the range of 1.7–2.2 Å, and are of moderate to weak nature and contributed mainly by electrostatic interaction.[65] All structures are rendered in PyMol (Fig. 16).

In the case of baicalein, cluster analysis showed two major clusters with 23 and 28 structures having the lowest binding energies −8.28 kcal mol^{-1} and −8.11 kcal mol^{-1}. The docking poses of baicalein in these two clusters are flipped to each other, both in the AATT pocket. Baicalein formed two hydrogen bonds; one with adenine (N3H of A4; 1.9 Å) and with sugar-phosphate backbone of thymine bases (O4′ of T5, 2 Å).

Chrysin showed similar binding with octamer DNA and two clusters with 20 and 33 conformations. The structure with the lowest binding energy −8.74 kcal mol^{-1} formed two hydrogen bonds between O1of chrysin with N3H of A4 (1.78 Å) and 7OH of chrysin with O2 of T14 (1.795 Å).

Two major clusters were found for flavone; 30 and 65 conformations, each with binding energies −8.46 kcal mol^{-1}, −8.21 kcal mol^{-1}, respectively. Though flavone showed binding energy closer to baicalein, no H bond was observed to be formed between flavone and DNA in the most populated cluster (65 conformations), and the intermolecular energy was slightly higher for flavone. O1 of flavone is found to make H bond with O2 of T13 residue (2.92 Å) of octamer DNA.

Different interactions involved in the complexes are depicted in Fig. 17A–C using Ligplot+.[66] Both baicalein and chrysin have equivalent binding sites (red colour bonded residues), whereas flavone showed no equivalent binding sites. Ligplot illustrated the hydrophobic interactions involved in forming and stabilizing the DNA–ligand complexes (Fig. 17D). All three compounds are oriented in a similar fashion when bound to the DNA (Fig. 17D).

6.2 With 1BNA

Four hydrogen bonds were formed between baicalein and dodecamer DNA, *viz.*, O1 of baicalein with O4 of T8 and N3 of A18, O4 with O3′ (backbone) of T19, 5OH with O3′ (backbone) of T19 and 7OH with O4′ (sugar ring) of T8. The lowest energy cluster consisted of 15 structures, and the lowest energy in this cluster was −8.33 kcal mol^{-1}.

Chrysin formed six hydrogen bonds with 1BDNA, *viz.*, O1 of chrysin with N3 of A18, O4 with O3′ of C9, 5OH with O3′ and O5′ of C9 (backbone), 7OH with N3 of A17 and O4′ of A18 sugar ring. The lowest energy in the cluster having 30 structures was −8.61 kcal mol^{-1}. Three hydrogen bonds are observed with flavone; between O4 of flavone and DNA, *viz.*, N3 of A17, O4′ of A18 sugar ring, and O2 of C9. The lowest energy in the cluster with 60 structures was −8.22 kcal mol^{-1}. Docked poses are shown in Fig. 18. Ligplot shown in Fig. 19A–C portrays the interactions involved. The docking poses show that baicalein and chrysin's orientations are similar while flavone is flipped by 180° (Fig. 19D).

The molecular modelling analysis reveals that all three compounds are located near the AT rich region in the case of both DNA sequences. With both DNA sequences, it is observed that the flavone compounds form hydrogen bonds with the base and the sugar backbone. Atoms present in the minor groove region (N3 of A and O2 of T) are involved in the hydrogen bonds, confirming that they are bound in the minor groove region. The negative binding energy ensures that the interaction between the three flavone compounds and DNA sequences is

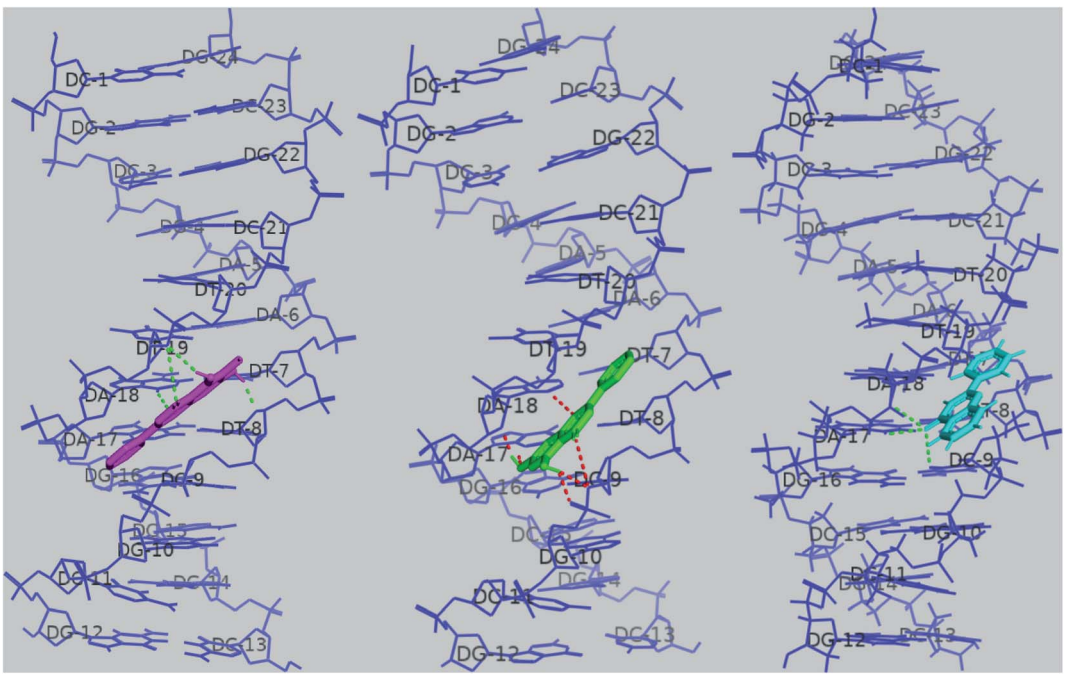

Fig. 18 Docked poses of baicalein (magenta), chrysin (green) and flavone (cyan) with 1BNA. Hydrogen bonds are shown as dashed lines.

Open Access Article. Published on 01 September 2021. Downloaded on 4/7/2026 8:03:30 PM.
This article is licensed under a Creative Commons Attribution-NonCommercial 3.0 Unported Licence.

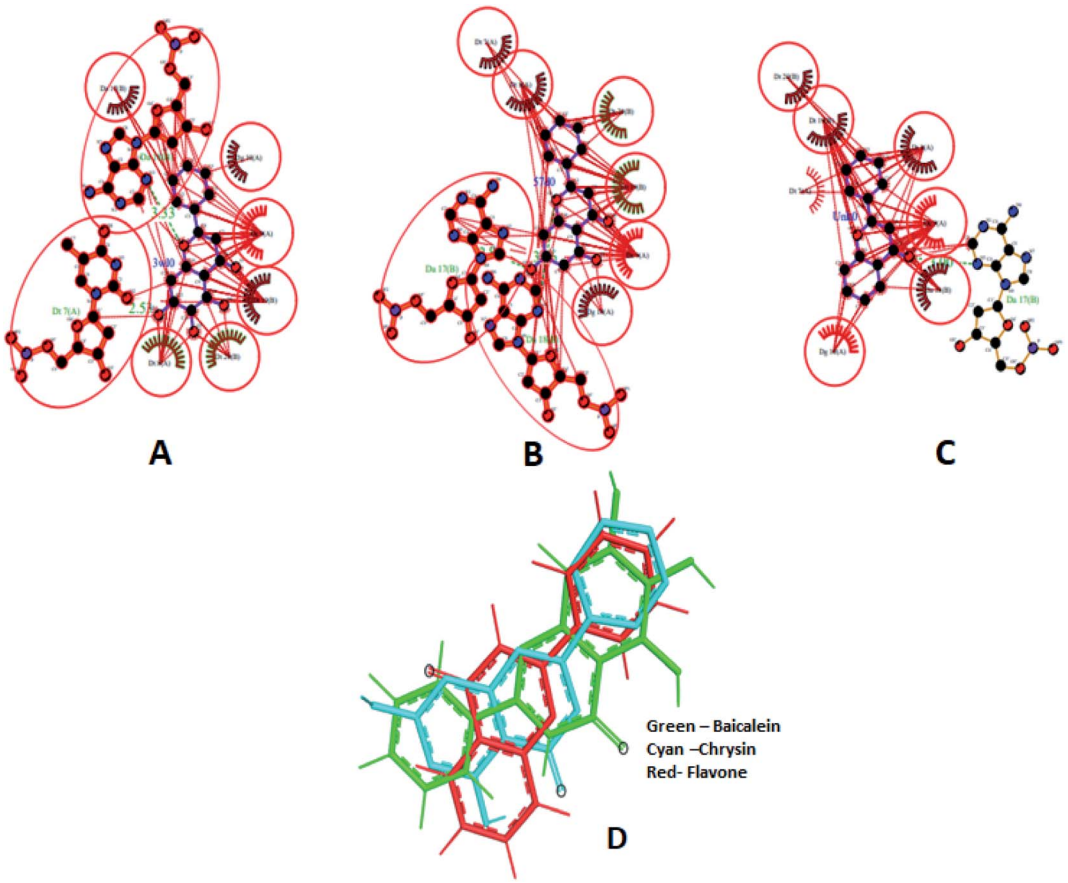

Fig. 19 Ligplot showing the interactions of baicalein (3w10) (A), chrysin (57d0) (B) and flavone (Unk0) (C) with 1BNA. Hydrophobic interactions are shown as red lines, hydrogen bond interactions are in green, red circles and ellipses shows the equivalent sites among three complexes, thick red bonds represent equivalent residues involved in hydrophobic interaction. Docked poses of baicalein, chrysin and flavone superimposed (D).

thermodynamically favorable. Thus, these molecular docking data suggest that the flavones bind to DNA through groove modes of binding and are near the AT region. Vitorino *et al.*[13] reported similar findings that hydroxyflavones exhibit external binding to DNA by forming hydrogen bonds with the DNA backbone's phosphate groups.

These results are not in line with the results of Tu *et al.*[21] Therefore, we studied interactions of these flavones with few other DNA sequences. Docking of all three compounds with DNA sequences $d(CGATCG)_2$ (PDB:1Z3F), $d(CGTACG)_2$ (PDB:1K2K), $d(CACGTG)_2$ (PDB:1UQC), $d(TGATCA)_2$ (PDB:1SY8), $d(CGAATTCG)_2$ (PDB:1BNA), $d(CGTTAACG)_2$ (PDB:1CQO), $d(CGCGATATCGCG)_2$ (PDB:1VTJ), were performed. The results showed that the flavones intercalated into the DNA bases only in the case of $d(CGATCG)_2$, and in all other cases, it is binding externally to/near the AT regions. The docked poses are depicted in ESI Fig. 11A–G.† Many anticancer drugs such as daunorubicin, doxorubicin, adriamycin bind to the 5′-CpG 3′ sequence through intercalation.[67–70] Docking results are not in agreement with the experimental data. This may be due to the reason that the experiments were performed in an aqueous environment whereas docking was performed in the absence of a water shell.

Flavones are reported to possess anticancer activity. Therefore, one of the possible mechanisms of their anticancer activity can be correlated to the intercalation of these molecules into the $d(CGATCG)_2$ sequence and their partial intercalation to other DNA sequences. Also, it is known that type-2 restriction enzyme Pvu-1 recognizes the DNA sequence $d(CGATCG)_2$.[71] This hints that flavones may able to block Pvu-1 from binding to the DNA. Experimental data, as well as the docking results, indicate the possibility that they can alter or block the binding of many AT region binding proteins such as TATA box binding protein (TBP), male sex determining factor (SRY).[72] These results open the door for examining the mechanism of flavones' therapeutic activity to understand their role and other potential targets in the cell.

7. Conclusion

In the reported work, we attempted to examine the DNA binding activity of baicalein, chrysin and flavone. Biophysical techniques and molecular modelling studies unveiled the interaction of these compounds with CT DNA and the sequence $d(CCAATTGG)_2$. The changes in the melting temperatures of DNA in the free form and complex form with compounds were significant enough to predict for intercalative mode of binding.

© 2021 The Author(s). Published by the Royal Society of Chemistry

Open Access Article. Published on 01 September 2021. Downloaded on 4/7/2026 8:03:30 PM.
This article is licensed under a Creative Commons Attribution-NonCommercial 3.0 Unported Licence.

The stability of the complex was high for baicalein, followed by chrysin. Flavone formed a very weak complex. The changes in absorption spectra also support the mode of binding. CD studies confirmed the intercalation of the compounds resulting in large conformational changes of DNA. Absence of induced CD band hints that the compounds may be partially intercalated or intercalated in a tilted direction. Displacement assays shows that the compounds were able to displace EtBr and Hoechst to some extent. Molecular docking studies with different DNA sequences show that the molecules are bound near the AT region of the sequences in a groove binding mode, except with $d(CGATCG)_2$. The discrepancy in the docking result can be due to the absence of an aqueous environment. In the case of $d(CGATCG)_2$, the compounds are in the intercalated form, which agrees with the literature reports. This result hints that the three flavone compounds can be used for sequence-specific targeting and point to the potential use of them as drug-like molecules.

Author contributions

Shailendra Kumar collected experimental data, analyzed and wrote the initial draft. Maya S Nair conceptualized, designed experiments, interpreted data, and edited the manuscript.

Conflicts of interest

The authors declare that they have no competing financial interest or personal relationship that could have appeared to influence the work reported in this paper.

Acknowledgements

Shailendra Kumar gratefully acknowledges University Grant Commission (UGC), India for a student research fellowship. Maya S Nair is grateful to the Council of Scientific and Industrial Research (CSIR), India for partial funding.

References

1 R. Palchaudhuri and P. J. Hergenrother, DNA as a target for anticancer compounds: methods to determine the mode of binding and the mechanism of action, *Curr. Opin. Biotechnol.*, 2007, **18**, 497–503.
2 W. D. Wilson and R. L. Jones, Intercalating drugs: DNA binding and molecular pharmacology, *Adv. Pharmacol. Chemother*, 1981, **18**, 177–222.
3 S. Neidle, *Cancer drug design and discovery*, Elsevier, 2011.
4 C. M. Nunn, E. Garman and S. Neidle, Crystal structure of the DNA decamer d(CGCAATTGCG) complexed with the minor groove binding drug netropsin, *Biochemistry*, 1997, **36**, 4792–4799.
5 F. A. Tanious, T. C. Jenkins, S. Neidle and W. D. Wilson, Substituent position dictates the intercalative DNA-binding mode for anthracene-9,10-dione antitumor drugs, *Biochemistry*, 1992, **31**, 11632–11640.
6 J. Bhattacharyya, A. Basu and G. S. Kumar, Intercalative interaction of the anticancer drug mitoxantrone with double stranded DNA: A calorimetric characterization of the energetics, *J. Chem. Thermodyn.*, 2014, **75**, 45–51.
7 J. M. Gottesfeld, J. M. Turner and P. B. Dervan, Chemical approaches to control gene expression, *Gene Expr*, 2000, **9**(1–2), 77–91.
8 G. S. Khan, A. Shah, Z-ur. Rehman and D. Barker, Chemistry of DNA minor groove binding agents, *J. Photochem. Photobiol. B Biol.*, 2012, **115**, 105–118.
9 S. Bhaduri, N. Ranjan and D. P. Arya, An overview of recent advances in duplex DNA recognition by small molecules, *Beilstein J. Org. Chem.*, 2018, **14**, 1051–1086.
10 A. G. Atanasov, S. B. Zotchev, V. M. Dirsch, *et al.*, Natural products in drug discovery: advances and opportunities, *Nat. Rev. Drug. Discov.*, 2021, **20**, 200–216.
11 S. Banerjee, Z. Wang, M. Mohammad, F. H. Sarkar and R. M. Mohammad, Efficacy of selected natural products as therapeutic agents against cancer, *J. Nat. Prod.*, 2008, **71**, 492–496.
12 D. J. Newman and G. M. Cragg, Natural Products as Sources of New Drugs from 1981 to 2014, *J. Nat. Prod.*, 2016, **79**, 629–661.
13 J. Vitorino and M. J. Sottomayor, DNA interaction with flavone and hydroxyflavones, *J. Mol. Struct.*, 2010, **975**, 292–297.
14 C.-J. Hsieh, K. Hall, T. Ha, C. Li, G. Krishnaswamy and D. S. Chi, Baicalein inhibits IL-1beta- and TNF-alpha-induced inflammatory cytokine production from human mast cells via regulation of the NF-kappaB pathway, *Clin. Mol. Allergy*, 2007, **5**, 5.
15 P. Sithisarn, P. Rojsanga and P. Sithisarn, Inhibitory Effects on Clinical Isolated Bacteria and Simultaneous HPLC Quantitative Analysis of Flavone Contents in Extracts from Oroxylum indicum, *Molecules*, 2019, **24**, 10.
16 K. Zandi, B. T. Teoh, S. S. Sam, P. F. Wong, M. R. Mustafa and S. AbuBakar, Novel antiviral activity of baicalein against dengue virus, *BMC Complement. Altern. Med.*, 2012, **12**, 214.
17 H. C. Ahn, S. Y. Lee, J. W. Kim, W. S. Son, C. G. Shin and B. J. Lee, Binding aspects of baicalein to HIV-1 integrase, *Mol. Cells*, 2001, **12**, 127–130.
18 S. Samarghandian, J. T. Afshari and S. Davoodi, Chrysin reduces proliferation and induces apoptosis in the human prostate cancer cell line pc-3, *Clinics*, 2011, **66**, 1073–1079.
19 D. Y. Zhang, J. Wu, F. Ye, L. Xue, *et al.*, Inhibition of cancer cell proliferation and prostaglandin E2 synthesis by Scutellaria baicalensis, *Cancer Res.*, 2003, **63**, 4037–4043.
20 N. Cotelle, J. L. Bernier, J. P. Catteau, J. Pommery, J. C. Wallet and E. M. Gaydou, Antioxidant properties of hydroxy-flavones, *Free Radic. Biol. Med.*, 1996, **20**, 35–43.
21 B. Tu, Z. F. Chen, Z. J. Liu, L. Y. Cheng and Y. J. Hu, Interaction of flavones with DNA in vitro: Structure-activity relationships, *RSC Adv.*, 2015, **5**, 33058–33066.
22 M. Rossi, R. Meyer, P. Constantinou, *et al.*, Molecular structure and activity toward DNA of baicalein, a flavone

Open Access Article. Published on 01 September 2021. Downloaded on 4/7/2026 8:03:30 PM.
This article is licensed under a Creative Commons Attribution-NonCommercial 3.0 Unported Licence.

constituent of the Asian herbal medicine 'Sho-saiko-to, *J. Nat. Prod.*, 2001, **64**, 26–31.

23 G. Meng, W. Shumin, W. Jiali, L. Dan, G. Qingyu and L. Limin, Spectroscopic and Electrochemical Methods on the Interaction Mechanism of Baicalein with DNA, *Chinese Journal of Applied Chemistry*, 2014, **31**, 114–119.

24 Y. Sun, S. Bi, D. Song, C. Qiao, D. Mu and H. Zhang, Study on the interaction mechanism between DNA and the main active components in Scutellaria baicalensis Georgi, *Sens. Actuators, B*, 2008, **129**, 799–810.

25 P. P. Kuang, M. Joyce-Brady, X. H. Zhang, J. C. Jean and R. H. Goldstein, Fibulin-5 gene expression in human lung fibroblasts is regulated by TGF-β and phosphatidylinositol 3-kinase activity, *Am. J. Physiol. Cell Physiol.*, 2006, **291**, 1412–1421.

26 S. Abhiman, L. M. Iyer and L. Aravind, BEN: A novel domain in chromatin factors and DNA viral proteins, *Bioinformatics*, 2008, **24**, 458–461.

27 T. Matsubasa, M. Takiguchi, I. Matsuda and M. Mori, Rat Argininosuccinate Lyase Promoter: The Dyad-Symmetric CCAAT Box Sequence CCAATTGG in the Promoter Is Recognized by NF-Y 1, *J. Biochem.*, 1994, **116**, 1044–1055.

28 J. B. Park and M. Levine, Characterization of the promoter of the human ribonucleotide reductase R2 gene, *Biochem. Biophys. Res. Commun.*, 2000, **267**, 651–657.

29 P. Borger, H. Matsumoto, S. Boustany, *et al.*, Disease-specific expression and regulation of CCAAT/enhancer-binding proteins in asthma and chronic obstructive pulmonary disease, *J. Allergy Clin. Immunol.*, 2007, **119**, 98–105.

30 C. Santoro, N. Mermod, P. C. Andrews and R. Tjian, A family of human CCAAT-box-binding proteins active in transcription and DNA replication: cloning and expression of multiple cDNAs, *Nature*, 1988, **334**, 218–224.

31 G. M. Morris, R. Huey, W. Lindstrom, *et al.*, AutoDock4 and AutoDockTools4: Automated docking with selective receptor flexibility, *J. Comput. Chem.*, 2009, **30**, 2785–2791.

32 N. M. O'Boyle, M. Banck, C. A. James, C. Morley, T. Vandermeersch and G. R. Hutchison, Open Babel: An open chemical toolbox, *J. Cheminform*, 2011, **3**, 33.

33 *The PYMOL Molecular Graphics System, Version 2.4.1*, Schrodinger, LLC.

34 R. Kanwal, M. Datt, X. Liu and S. Gupta, Dietary flavones as dual inhibitors of DNA methyltransferases and histone methyltransferases, *PLoS One*, z2016, **11**, e0162956.

35 A. S. Meyer and G. H. Ayres, The Mole Ratio Method for Spectrophotometric Determination of Complexes in Solution1, *J. Am. Chem. Soc.*, 1957, **79**, 49–53.

36 F. Barcelo and J. Portugal, Berenil recognizes and changes the characteristics of adenine and thymine polynucleotide structures, *Biophys. Chem.*, 1993, **47**, 251–260.

37 M. B. Gholivand, S. Kashanian, H. Peyman and H. Roshanfekr, DNA-binding study of anthraquinone derivatives using Chemometrics methods, *Eur. J. Med. Chem.*, 2011, **46**, 2630–2638.

38 P. J. Cox, G. Psomas and C. A. Bolos, Characterization and DNA-interaction studies of 1,1-dicyano-2,2-ethylene dithiolate Ni(II) mixed-ligand complexes with 2-amino-5-methyl thiazole, 2-amino-2-thiazoline and imidazole. Crystal structure of [Ni(i-MNT)(2a-5mt)2], *Bioorg. Med. Chem.*, 2009, **17**, 6054–6062.

39 N. Shahabadi, S. Kashanian and F. Darabi, DNA binding and DNA cleavage studies of a water soluble cobalt(II) complex containing dinitrogen Schiff base ligand: The effect of metal on the mode of binding, *Eur. J. Med. Chem.*, 2021, **45**, 4239–4245.

40 J. D. McGhee and P. H. von Hippel, Theoretical aspects of DNA-protein interactions: Co-operative and non-co-operative binding of large ligands to a one-dimensional homogeneous lattice, *J. Mol. Biol.*, 1974, **86**, 469–489.

41 I. Piantanida, L. Mašić and G. Rusak, Structure-spectrophotometric selectivity relationship in interactions of quercetin related flavonoids with double stranded and single stranded RNA, *J. Mol. Struct.*, 2009, **924–926**, 138–143.

42 R. C. Yadav, G. S. Kumar, K. B. Prabal Giri, *et al.*, Berberine, a strong polyriboadenylic acid binding plant alkaloid: spectroscopic, viscometric, and thermodynamic study, *Bioorg. Med. Chem.*, 2005, **13**, 165–174.

43 A. M. Pyle, J. P. Rehman, R. Meshoyrer, C. V. Kumar and N. J. Turro, Mixed-ligand complexes of ruthenium(II): Factors governing binding to DNA, *J. Am. Chem. Soc.*, 1989, **111**, 3051–3058.

44 A. G. Krishna, D. V. Kumar, B. M. Khan, S. K. Rawal and K. N. Ganesh, Taxol–DNA interactions: fluorescence and CD studies of DNA groove binding properties of taxol, *Biochim. Biophys. Acta Gen. Subj.*, 1998, **1381**, 104–112.

45 S. Bi, C. Qiao, D. Song, *et al.*, Study of interactions of flavonoids with DNA using acridine orange as a fluorescence probe, *Sens. Actuators, B*, 2006, **119**, 199–208.

46 C. Ji, X. Yin, H. Duan and L. Liang, Molecular complexes of calf thymus DNA with various bioactive compounds: Formation and characterization, *Int. J. Biol. Macromol.*, 2021, **168**, 775–783.

47 K. Bhadra and G. S. Kumar, Interaction of berberine, palmatine, coralyne, and sanguinarine to quadruplex DNA: a comparative spectroscopic and calorimetric study, *Biochim. Biophys. Acta*, 2011, **1810**, 485–496.

48 J. Olmsted and D. R. Kearns, Mechanism of ethidium bromide fluorescence enhancement on binding to nucleic acids, *Biochemistry*, 1977, **16**, 647–3654.

49 C. E. Bostock-Smith and M. S. Searle, DNA minor groove recognition by bis-benzimidazole analogues of Hoechst 33258: insights into structure-DNA affinity relationships assessed by fluorescence titration measurements, *Nucleic Acids Res.*, 1999, **27**, 1619–1624.

50 Y. Guan, W. Zhou, X. Yao, M. Zhao and Y. Li, Determination of nucleic acids based on the fluorescence quenching of Hoechst 33258 at pH 4.5, *Anal. Chim. Acta*, 2006, **570**, 21–28.

51 V. Nikolai, Binding of Hoechst with nucleic acids using fluorescence spectroscopy, *J. Biophys. Chem.*, 2011, **2**, 443–447.

52 D. Sahoo, P. Bhattacharya and S. Chakravorti, Quest for Mode of Binding of 2-(4- (Dimethylamino)styryl)-1-methylpyridinium Iodide with Calf Thymus DNA, *J. Phys. Chem. B*, 2010, **114**, 2044–2050.

© 2021 The Author(s). Published by the Royal Society of Chemistry

Open Access Article. Published on 01 September 2021. Downloaded on 4/7/2026 8:03:30 PM.
This article is licensed under a Creative Commons Attribution-NonCommercial 3.0 Unported Licence.

53 D. Sarkar, P. Das, S. Basak and N. Chattopadhyay, Binding Interaction of Cationic Phenazinium Dyes with Calf Thymus DNA: A Comparative Study, *J. Phys. Chem. B*, 2008, **112**, 9243–9249.

54 J. B. LePecq and C. Paoletti, A fluorescent complex between ethidium bromide and nucleic acids. Physical-chemical characterization, *J. Mol. Biol.*, 1967, **827**, 7–106.

55 C. Qiao, S. Bi, Y. Sun, D. Song, H. Zhang and W. Zhou, Study of interactions of anthraquinones with DNA using ethidium bromide as a fluorescence probe, *Spectrochim. Acta Part A Mol. Biomol. Spectrosc.*, 2008, **70**, 136–143.

56 A. A. Saboury and A. A. Moosavi-Movahedi, Clarification of calorimetric and van't hoff enthalpies for evaluation of protein transition states, *Biochem. Educ.*, 1994, **22**, 210–211.

57 F. P. Schwarz, K. Puri and A. Surolia, Thermodynamics of the binding of galactopyranoside derivatives to the basic lectin from winged bean (Psophocarpus tetrogonolobus), *J. Biol. Chem.*, 1991, **266**, 24344–24350.

58 J. Kypr, I. Kejnovská, D. Renčiuk and M. Vorlíčková, Circular dichroism and conformational polymorphism of DNA, *Nucleic Acids Res.*, 2009, **37**, 1713–1725.

59 M. M. Islam, M. Chakraborty, P. Pandya, A. Al Masum, N. Gupta and S. Mukhopadhyay, Binding of DNA with Rhodamine B: Spectroscopic and molecular modeling studies, *Dyes Pigm.*, 2013, **99**, 12–422.

60 B. Nguyen, D. Homelberg, C. Bailly, *et al.*, Characterization of a Novel DNA Minor-Groove Complex, *Biophys. J.*, 2004, **86**, 1028–1041.

61 Y.-M. Chang, C. K.-M. Chen and M.-H. Hou, Conformational Changes in DNA upon Ligand Binding Monitored by Circular Dichroism, *Int. J. Mol. Sci.*, 2012, **13**, 3394–3413.

62 I. Piantanida, B. S. Palm, Z. Mladen and H.-J. Schneider, A new 4, 9-diazapyrenium intercalator for single-and double-stranded nucleic acids: distinct differences from related diazapyrenium compounds and ethidium bromide, *J. Chem. Soc. Perkin Trans.*, 2001, **9**, 1808–1816.

63 H. Xu, K. C. Zheng, Y. Chen, *et al.*, Effects of ligand planarity on the interaction of polypyridyl Ru(ii) complexes with DNA, *Dalt. Trans.*, 2003, **11**, 2260–2268.

64 T. Šmidlehner, I. Piantanida and G. Pescitelli, Polarization spectroscopy methods in the determination of interactions of small molecules with nucleic acids - tutorial, *Beilstein J. Org. Chem.*, 2018, **4**, 84–105.

65 G. A. Jeffrey, *An Introduction to Hydrogen Bonding*, Oxford University Press, New York, 1997.

66 R. A. Laskowski and M. B. Swindells, LigPlot+: multiple ligand-protein interaction diagrams for drug discovery, *J. Chem. Inf. Model.*, 2011, **51**, 2778–2786.

67 A. H.-J. Wang, Intercalative drug binding to DNA, *Curr. Opin. Struct. Biol.*, 1992, **2**, 361–368.

68 B. Jawad, L. Poudel, R. Podgornik, N. F. Steinmetz and W.-Y. Ching, Molecular mechanism and binding free energy of doxorubicin intercalation in DNA, *Phys. Chem. Chem. Phys.*, 2019, **21**, 3877–3893.

69 A. H. Wang, G. Ughetto, G. J. Quigley and A. Rich, Interactions between an anthracycline antibiotic and DNA: molecular structure of daunomycin complexed to d(CpGpTpApCpG) at 1.2-A resolution, *Biochemistry*, 1987, **26**, 1152–1163.

70 S. Mazzini, R. Mondelli and E. Ragg, Structure and dynamics of intercalation complexes of anthracyclines with $d(CGATCG)_2$ and $d(CGTACG)_2$. 2D-^{1}H and ^{31}P NMR investigation**s**, *J. Chem. Soc., Perkin Trans.*, 1998, **2**, 1983–1992.

71 https://www.Uniprot.org/uniport/P31031.

72 C. A. Bewley, A. M. Gronenborn, and G. M. Clore, Minor Groove-Binding Architectural Proteins: Structure, Function, and DNA Recognition, in *Annual Reviews Collection*, National Center for Biotechnology Information (US), Bethesda (MD), 2002.